

RESTAURANT FOOD WASTE MANAGEMENT  
USING MICROWAVE PLASMA GASIFICATION  
TECHNOLOGY

VIJAYAKUMAR KARUNAMOOTHEI

A thesis submitted in partial fulfillment of the  
requirements of Liverpool John Moores University  
for the degree of  
Doctor of Philosophy

MAY 2018

# DECLARATION

The research reported in this thesis was conducted at Liverpool John Moores University, Department of Built & Environment , at Built Environment and Sustainable Technologies Research Institute (BEST). I declare that presented work is my own and has not been submitted for a degree at another university.

VIJAYAKUMAR KARUNAMOOTHEI

Liverpool John Moores University

MAY 2018

# ACKNOWLEDGMENT

I would like to express my sincere gratitude for the friendships and support that has made my time here at Liverpool John Moores University (LJMU) the most rewarding experience. This research and dissertation would not have been possible without the countless individuals who have both inspired and supported me along the way. I can safely say that I would not have been successful without their precious support. First, I would like to gather hands to the almighty **GOD, My father, mother, sister and brothers** for enabling me to complete my PhD thesis successfully. In addition, I would like to express my sincere gratitude and appreciation to the following persons; if any have been forgotten, please accept my sincerest of apologies:

- I owe my deepest gratitude to my director of studies Dr Stephen Wylie for his expert advice and support throughout my research.
- I owe my deepest gratitude to my supervisor, Professor Andy Shaw, Head of the BEST Research Institute, for his excellent supervision, guidance and encouragement throughout this work. Furthermore, Prof Andy and Dr Stephen have been an excellent mentor and a constant source of knowledge, motivation and encouragement throughout my graduate studies.
- I would like to convey my deepest gratitude to Professor Ahmed Al-Shamma'a, Dean of the Faculty of Technology and Environment, for the opportunity of undertaking this PhD. Prof has given the lecture about electromagnetic waves propagation and antenna in my MSc studies.

- A big thank you goes to my follow research friends Alex and Malarvili for their guidance, advice and continual help throughout this research.
- I also would like to acknowledge the assistance and friendship of all the lecturers, researchers, technicians and administrative staff in the Department of Built and Environment Engineering, Liverpool John Moores University, especially those directly involved with this research. Their enthusiasm and encouragement have made my research enjoyable and memorable. I would also like to thank the many individuals at the BEST Research Institute, Liverpool John Moores University for all their help. Last, but not least, the preparation of the project report is a time-consuming task, requiring many hours of effort. I would also like to express my deepest appreciation to my beloved brothers and sisters at Preston, friends who have been supportive and understanding during my studies.

## ABSTRACT

The novelty of this research is that it investigates an on-site solution for the treatment of restaurant waste using a microwave generated plasma for pyrolysis and gasification. The developed system has been used to treat waste from a city centre fast food restaurant. The system was designed with the aim of reducing the amount of waste being sent to landfill by approximately 94%. The waste is mostly food based but also includes paper waste such as napkins. It was separated into three categories: mixed food, paper and fries. Samples of the mixed food and paper waste were analysed for chemical composition and calorific value.

A 2.45GHz magnetron was used to supply 1kW of microwave power to a plasma cavity that had an argon flow rate of 1.5 litre per minute. The design of the microwave plasma cavity was performed using the simulation software, COMSOL. The cavity consists of a tapered waveguide section that is shorted at one end to produce a stationary wave with a large electric field at the gas nozzle. The field is strong enough to produce a self-striking argon plasma when the power is applied. Nitrogen was used to keep the plasma cavity clear of smoke, vapours and other hot gas. The best nitrogen flow rates were found to be around 2 litres/minute, although 5 litres/minute was used in the test to avoid the CO sensor saturating. The combination of the argon and nitrogen was used to purge the gasifier of oxygen. The pressure inside the gasifier was held at 200mbar during the experiments.

The resulting plasma jet was used to produce syngas from the waste samples inside a thermally insulated, steel-walled reactor. Temperature profiles were recorded to find the best gas flow rates. 10g samples of the three waste categories were tested in triplicate and the results are presented.

Syngas production was recorded using a Quintox gas analyser that measured CO, CO<sub>2</sub> and O<sub>2</sub>. The data was captured every 10s during testing using a PC running a custom-built LabVIEW program. This program was also used to set the microwave output power and record the reflected power and temperatures using National Instruments cDAQ modules with analogue to digital converters. The CO and H<sub>2</sub> in syngas can be used as a fuel to offset the cost of running the plasma jet.

The results reveal that it is possible to generate the syngas using waste food materials. This study has included an investigation of some of the parameters, including power and flow rates of argon and nitrogen, on the plasma created. Others effects were taken into consideration throughout the research such as the study of the sample moisture levels and the final reduction of mass after the experiment.

The ashes produced by the tests were investigated using SEM/EDX analysis. These results are also presented and analysed.

# LIST OF CONTENTS

DECLARATION .....	i
ACKNOWLEDGMENT .....	ii
ABSTRACT .....	iv
LIST OF CONTENTS.....	vi
LIST OF FIGURES .....	x
LIST OF TABLES.....	xiv
1: INTRODUCTION .....	1
1.1 Introduction .....	1
1.2 Restaurant waste .....	5
1.3 Current on-site state of the art equipment.....	6
1.4 Aim and objectives of the research .....	9
1.5 Aim.....	9
1.6 Objectives .....	9
1.7 Details of objectives:.....	9
1.8 Chapter Summary .....	11
2 : WASTE MANAGEMENT AND TREATMENT .....	12
2.1 Introduction .....	12
2.2 Prevention.....	15

2.3	Reuse .....	15
2.4	Recycle .....	15
2.5	Recovery.....	15
2.5.2	Existing Technologies advantages and limitations. ....	21
2.6	Chapter Summary.....	22
3	: Electromagnetic Radiation .....	23
3.1	Microwaves .....	23
3.2	Waveguide Transmission.....	25
3.2.1	Cut-off Frequency.....	29
3.3	Chapter Summary.....	31
4	: Introduction .....	32
4.1	Plasma Excitation Sources .....	33
4.2	Gas Interaction with Microwaves .....	33
4.3	Key Microwave Plasma Gasification Parameters .....	35
4.4	Microwave Plasma Cavity Modelling .....	37
4.5	Microwave plasma gasification system .....	41
4.6	Gasification Reactor.....	44
4.7	Gas Feed Control .....	44
4.8	Self-striking plasma .....	45
4.9	Temperature Thermocouples.....	45
4.10	Power Control .....	47

4.11	Quartz Window .....	48
4.12	Nozzle.....	49
4.13	Quintox Gas Analyser Sensor.....	50
4.14	Health and Safety for CO.....	51
4.15	Chapter Summary.....	52
5	: Introduction .....	53
5.1	Sample preparation .....	53
5.2	Samples Properties Determination .....	56
5.3	Food Waste Analysis .....	56
5.4	Microwave-induced plasma gasifier .....	58
5.5	System Experimentation and Parameters.....	60
5.5.1	Power .....	60
5.5.2	Gas Flow Rate.....	61
5.5.3	Pressure.....	62
5.6	Plasma Temperature Profile .....	63
5.7	Gas analysis .....	65
5.8	Chapter Summary.....	66
6	: Introduction .....	68
6.1	Sample Moisture Properties.....	70
6.2	System Experimentation .....	72
6.2.1	EDX for Results for Mix Food Waste.....	74

6.2.2	EDX Result for Paper/Napkin Waste.....	75
6.2.3	EDX Result for Fries/Chips Waste .....	77
6.3	Plasma Treatment of Waste .....	78
6.3.1	Gas Analysis .....	80
6.3.2	Mixed Food Results.....	81
6.3.3	Fries .....	84
6.3.4	Paper/Napkin .....	87
6.3.5	Mass Measurements Mixed Food .....	90
6.3.6	Mass Measurements Fries/Chips .....	92
6.3.7	Mass Measurements Paper/Napkin Waste. ....	93
6.4	Chapter Summary.....	94
7	: Conclusion.....	95
7.1	Future Work.....	96
8	: References .....	99

# LIST OF FIGURES

Figure 1.1: Food Waste Hierarchy .....	3
Figure 1.2: Waste2O bio-digester ( <a href="http://www.waste2-0.com">http://www.waste2-0.com</a> ).....	6
Figure 2.1: Landfill Site. ....	12
Figure 2.2: Food Waste Hierarchy .....	14
Figure 3.1:EM Wave Classification [51] .....	23
Figure 3.2: Potential difference in waveguide .....	26
Figure 3.3: Movement of Electric 'E' and Magnetic 'H' fields inside a waveguide .....	26
Figure 3.4: Examples of Transmission Modes in Waveguides.....	28
Figure 3.5: Inside a waveguide (TE <sub>10</sub> ).....	29
Figure 3.6: Concept of Cut-off Frequency .....	30
Figure 4.1: States of the matter[58].....	32
Figure 4.2: Plasma Cavity Design.....	36
Figure 4.3: Two-sided taper design.....	37
Figure 4.4: Double sided taper design .....	37
Figure 4.5: E- field simulation for the TE <sub>101</sub> mode in WG9A waveguide.....	38
Figure 4.6: E- field magnitude for the TE <sub>101</sub> mode in WG9A waveguide .....	39
Figure 4.7: E- Field simulation for the TE <sub>102</sub> mode in WG9A waveguide .....	39
Figure 4.8: Travelling wave with short circuit at far end .....	40

Figure 4.9: Simulation of waveguide with the nozzle .....	41
Figure 4.10: Block diagram of the experimental set-up.....	41
Figure 4.11: Microwave plasma gasification system. ....	42
Figure 4.12: Gasification reactor and plasma cavity. ....	43
Figure 4.13: K-type thermocouple.....	45
Figure 4.14: Infra-red images of the gasifier and plasma cavity.....	46
<i>Figure 4.15 : Cdaq 9172 and Cseries compatible modules (ni.com).....</i>	<i>46</i>
Figure 4.16: (a) NI units for the power control (b) NI units for the temperature control .....	47
Figure 4.17: Microwave Window .....	48
Figure 4.18: Nozzle overview.....	49
Figure 4.19: Quintox 9106 Gas Analyser .....	50
Figure 5.1: Waste sample .....	53
Figure 5.2: Sample after grinding process. ....	55
<i>Figure 5.3: Samples inside drying Oven .....</i>	<i>56</i>
Figure 5.4: Microwave plasma gasifier.....	59
Figure 5.5: Microwave leakage detector .....	60
<i>Figure 5.6: 1kW Plasma in gasifier .....</i>	<i>62</i>
Figure 5.7: Plasma temperature profile at the box reactor .....	63
Figure 5.8: Temperature profile system .....	64

Figure 5.9: Temperatures recorded by the thermocouples under different power and flow rates .....	65
Figure 5.10: Drierite Unit .....	66
Figure 6.1: Samples before and after the gasification process. ....	72
Figure 6.2: EDX results for mixed food ash. ....	74
Figure 6.3: EDX results for Paper/Napkin ash. ....	75
Figure 6.4: EDX results for Fries/chip ash .....	77
Figure 6.5: Empty crucible weight .....	78
Figure 6.6: Crucible + sample weight .....	78
Figure 6.7: Dark yellow plasma .....	79
Figure 6.8: Vapour formation .....	79
Figure 6.9: Smoke formation .....	79
Figure 6.10: Flame reduced, more smoke .....	79
Figure 6.11: Reduced smoke .....	79
Figure 6.12: No visible smoke .....	79
Figure 6.13: Results for Mixed Food (1) .....	81
Figure 6.14: Results for Mixed Food (2) .....	82
<i>Figure 6.15: Results for Mixed Food (3) .....</i>	<i>83</i>
Figure 6.16: Results for Fries/Chip (1) .....	84
Figure 6.17: Results for Fries/Chip (2) .....	85
Figure 6.18: Results for Fries/Chip (3) .....	86

Figure 6.19: Results for Paper/Napkin (1).....	87
Figure 6.20: Results for Paper/Napkin (2).....	88
Figure 6.21: Results for Paper/Napkin (3).....	89

# LIST OF TABLES

Table 1.1: Restaurants in Liverpool One (November 2017).....	5
Table 1.2: Advanced Thermal Treatments.....	7
Table 2.1: Landfill Allowances for the UK .....	13
Table 2.2: Main Chemical reactions of gasification .....	18
Table 2.3: Syngas contaminant.....	19
Table 2.4: Main operating parameters for conventional, fast and flash pyrolysis[46, 47].....	20
Table 3.1: Waveguide Dimensions and their Operating Frequencies .....	25
Table 4.1: Gas sensor specification.....	50
Table 4.2: Parameters Outputted by Quintox 9106.....	51
<i>Table 5.1: Argon, Nitrogen and Temperature Profile Test .....</i>	<i>63</i>
Table 6.1: Food Waste Analysis .....	68
Table 6.2: Paper Waste Analysis .....	69
Table 6.3: Data obtained during drying process.....	70
Table 6.4: Moisture content calculation.....	71
Table 6.5: Ash content calculation .....	73
Table 6.6: Observation monitoring during the experiment .....	80
Table 6.7: Summary of the Total Gas Measurements.....	90

Table 6.8: Mass change of each mix food sample in response to microwave pyrolysis treatment.....	91
Table 6.9: Mass change of each fries/chips sample in response to microwave pyrolysis treatment.....	93
Table 6.10: Mass change of each napkin/paper waste sample in response to microwave pyrolysis treatment.....	94

# 1: INTRODUCTION

## 1.1 Introduction

According to the Waste and Resources Action Programme, (WRAP) [1, 2], the amount of waste generated every year by the food service industry is 3,415,000 tonnes, which includes approximately 600,000 tonnes of food waste from restaurants alone. Food waste rate in UK restaurants costs roughly 2-3% of their turnover according to The Sustainable Restaurant Association[3]. On-site shopping centre like at Liverpool One, have 33 food chains restaurants. Waste from Byron Hamburgers was used for experiment for this research. The influence of food waste on the environment is massive. When food is wasted all the carbon generated as it was produced, processed, transported and stored is also wasted. It is estimated that 20% of the United Kingdom's greenhouse emissions is related to this problem and this is equivalent to at least 15 million tonnes of carbon dioxide every year[4, 5].

Previous research conducted by *Lin* claims that most of the food wastes that is recycled is used for animal feed or is composted, the rest is incinerated or disposed of in landfill [6]. Disposing of food waste at landfill sites causes environmental impacts such as the production of large amounts of methane gas and the generation of landfill leachate, which is a liquid that drains from the waste and enters the environment [7, 8]. Furthermore, incineration of food waste can cause serious environmental problems according to *Mehmet* [9].

The main problem with the excess food is that it deteriorates quickly and becomes inedible. This makes collection, processing and transportation for

human consumption very difficult. WRAP claims that about two thirds of this waste is avoidable, and this is an issue that requires further investigation. A previous study conducted by *Lupa* claims that municipal solid waste (MSW), commercial and industrial waste (C&IW) has high energy content [10], which give an wide scope for this research to explore the potential return of the energy by using food waste. Ahmed and Gupta argued that waste food offers a good potential feedstock for power generation via gasification due to its high calorific value [11, 12]. According to *Caton et al*, dried food waste contains more energy than wood, which is more typical biomass fuel [13]. Syngas can be converted into electricity and valuable products, such as transportation fuels, fertilizers, chemicals or substitute natural gas[14, 15]. Thermal decomposition methods can solve two major problems, reduced the landfill volume and energy recovery [16]. This work, however, will focus on dealing with the considerable amount of food waste, and other biodegradable waste from restaurants, that is regarded as unavoidable. Disposing of this waste presents both a financial cost to the restaurant owners, in addition to its being an ecological issue. To address this issue, the waste hierarchy was introduced.

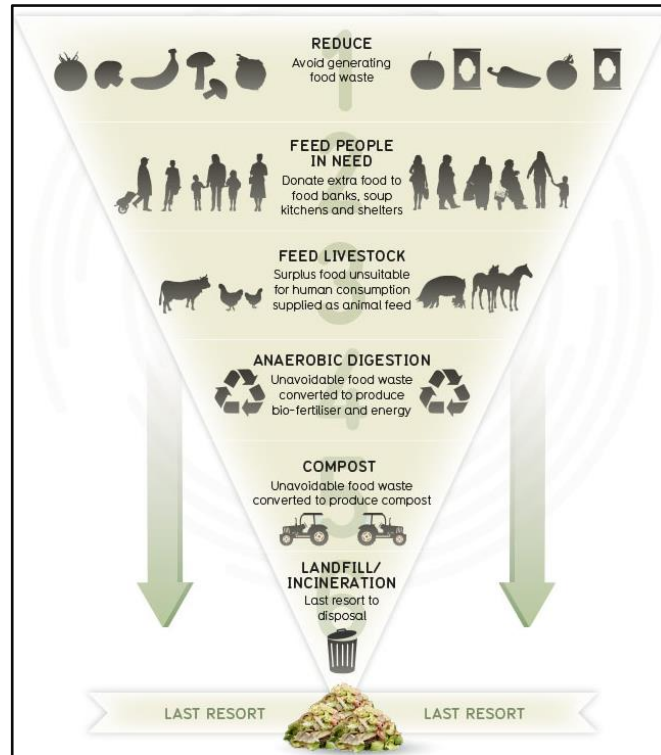


*Figure 0.1: Food Waste Hierarchy*

The waste hierarchy has been used in many countries to highlight the different options for waste management according to their environmental desirability. Figure 0.1 shows the breakdown of the hierarchy and further explanation is provided in Chapter 2. The hierarchy lists the solutions for the waste from the most desired to the least, and includes prevention, reuse, recycling, composting or anaerobic digestion, incineration and finally landfill.

This work focuses on the lower half of the hierarchy, and in particular on a novel on-site technique for the treatment of unavoidable waste from restaurants in built-up areas. Most of the current disposal methods are done offsite, and restaurants face an ever-increasing cost to transfer the waste, 60% of which is typically water [17]. Composting and anaerobic digestion (AD) are possible offsite solutions, for city based restaurants, that avoids landfill. Both

composting and AD require co-mixing with other waste streams to balance the nutrients within the food and enabling the microorganisms to break them down[18]. There are also limitations in the food that cannot be composted because meat, fish and cooked foods are not suitable for the composting process[19]. For AD, foods that contain relatively high amounts of sulphur, including fish and cabbage are not suitable due to the undesirable odours that are produced [20]. Both of these technologies are only economic as waste disposal option at larger scales and they also need to be located away from residential areas. Furthermore, previous research has mention that fuel gas can be produced from biomass and related material by gasification process to give a mixture of carbon monoxide, carbon dioxide, hydrogen and methane[21]. ***The novelty of this research is that it investigates an on-site solution for the treatment of restaurant waste using a microwave generated plasma for advanced thermal treatment.***

## 1.2 Restaurant waste

*Table 0.1: Restaurants in Liverpool One (November 2017)*

Barburrito	Bem Brasil	Bierkeller
Bill's	Browns	Byron
Chaophraya	Cosy Club	Cote Bistro
Ed's Easy Diner	Exchange at Hilton	Five Guys
Gourmet Burger Kitchen	Jamie's Italian	John Lewis Restaurant
Las Iguanas	Lunya	Nando's
Pizza Express	Pizza Hut Restaurants	Red's True BBQ
Roxy Ball Room	T.G.I Friday's	The Club House
Tortilla	Turtle Bay	Wagamama
Wahaca	Wok&Go	Yard & Coop
Yee Rah	YO! Sushi	Zizzi

Restaurants in built-up areas often belong to global chains. Typical examples can be found in the city centre of Liverpool, UK. Liverpool One is a 150,000 m<sup>2</sup> shopping and leisure complex, with over half a million visitors per week. It currently contains 33 restaurants, which are listed in Table 0.1. Although these are in a complex and the combined waste can be collected, they represent typical high street restaurant chains found throughout the UK.

For this research, the Byron Hamburger restaurant in Liverpool One has been chosen to represent a typical city centre restaurant. This particular restaurant been chosen because I am a member of staff there. This restaurant can generate up to 300kg of waste on a busy day.

### 1.3 Current on-site state of the art equipment

One commercially available on-site disposal method is Waste<sub>2</sub>O. This unit is manufactured by Mechline Developments in Milton Keynes, UK, and is shown in Figure 0.2: Waste<sub>2</sub>O bio-digester (<http://www.waste2-0.com>).



Figure 0.2: Waste<sub>2</sub>O bio-digester (<http://www.waste2-0.com>).

Waste<sub>2</sub>O is a bio-digester that has been designed to handle food waste. The manufacturers claim that it can digest up to 180kg of waste on-site per day, with all the waste occurring as effluent that flows down the drain and into sewerage system. This mean that there is no collection or landfill charges. The device requires approximately 600 litres of water per day at a constant 50°C,

which, assuming the mains water is at a temperature of 15°C, equates to an energy consumption of 24.4 kWhr per day. There is also an electrical input power of 1.1kW. The waste is broken down using poly-chips, supply by the manufactures, which impregnated with microorganisms. These poly-chips stay in the machine but need topping up over the course of its service life. The device can process soft, organic food waste such as fruit, vegetables, cooked and uncooked meat, fish, vegetables and fruit. However, it cannot process oils and fats, including butter and lard, bones, fruit seeds/stones, frozen or chilled food, raw dough, flours or yeast, eggshells or any hard fibrous foods.

The on-site approach proposed in this thesis will be able to deal with more of the waste streams list above by using an advanced thermal method. These methods heat the waste under reduced oxygen and include pyrolysis and gasification[22]. There properties are presented in Table 0.2.

*Table 0.2: Advanced Thermal Treatments*

<b>Technologies</b>	<b>Process</b>	<b>Temperature</b>	<b>Sources/Energy</b>
<b>Gasification</b>	Heated with little or no oxygen	>800°C	Syngas
<b>Pyrolysis</b>	Heated in the absence of oxygen	<500°C	Syngas gas, Char and Pyrolysis Oil

These two solutions are considered as energy-from-waste (EfW) technologies. Energy production from food waste (EfW) is a potential solution, due to its

relatively high calorific value [23]. It represents a feasible renewable energy path, and reduces the amount of waste being sent to landfill.

Syngas or synthesis gas [24, 25] is a fuel gas mixture consisting primarily of hydrogen, carbon monoxide and very often some carbon dioxide. Syngas is combustible and is often used as a fuel of internal combustion engines[26].

## 1.4 Aim and objectives of the research

### 1.5 Aim

The aim of this research is to investigate the novel use of a 2.45GHz microwave plasma to reduce the amount of restaurant waste sent to landfill by using thermal decomposition to produce syngas.

### 1.6 Objectives

- **Collect waste samples from a Byron Hamburgers restaurant at Liverpool One.**
- **Sent samples to external laboratory for analysis.**
- **Re-commission the existing 2.45GHz microwave plasma system to treat samples of the waste as a proposed on-site solution.**
- **Measure the gas output during the tests and monitor the initial mass of the sample and the mass of the solid residue after the test.**
- **Analyse the results and make recommendations for its use as an on-site technology for reducing landfill bound waste.**

### 1.7 Details of objectives:

1. Waste samples will be collected from a Byron Hamburger restaurant in Liverpool. The waste items will be separated into two different categories:
  - **Mixed food:** This includes bread, burgers, French fries and salads.
  - **Paper waste:** This includes napkins and greaseproof paper.

The waste from each category will be ground to a uniform consistency before processing.

2. Samples of both waste categories will be sent for chemical and calorific analysis at an external specialist laboratory.
3. An existing box-shaped reactor, designed to operate with a 2.45GHz microwave plasma system, will be re-commissioned. The reactor can be purged of oxygen, and it has a sight glass to allow the interaction between the plasma and the sample to be observed.
4. The output gas concentrations will be measured using a Quintox Gas Analyser (KM 9106). This unit is capable of measuring oxygen, carbon dioxide (CO<sub>2</sub>) and carbon monoxide (CO). A mixture of CO<sub>2</sub> and CO will be produced when the waste samples are heated by the plasma in the absence of oxygen inside the reactor. The initial mass of the sample and the mass of the solid residue after the experiment will also be collected.
5. The results obtained will be analysed and used to make necessary recommendations for the use of the plasma reactor as an on-site technology for reducing the landfill bound waste. A high ratio for CO/CO<sub>2</sub> will indicate that syngas production is occurring, and this could be used as a source of energy.

## 1.8 Chapter Summary

This chapter explains the background of food waste and the problems it presents. A solution is required to avoid all the waste generated being sent to landfill. This research focuses on restaurant waste from a built up area (Liverpool One retail centre). It describes the previous on-site solution, which was used for waste food treatment at Liverpool One and the drawbacks. Advanced thermal treatment is proposed as a solution. The research aims and objectives are discussed. Chapter Two will explain about the Waste Management and Treatment.

## 2 : WASTE MANAGEMENT AND TREATMENT

### 2.1 Introduction

Landfill sites such as that show in Table 2.1 cause air, water and soil pollution. They discharge carbon dioxide (CO<sub>2</sub>) and methane (CH<sub>4</sub>) into the atmosphere and chemicals (leachate) into the earth and groundwater [14].



*Figure 2.1: Landfill Site.*

(<http://www.sustainableglasgow.co.uk/news/category/recycling>)

The EU created the waste framework Directive (2008/98/EC)[27] to find alternative methods for managing waste, reducing landfill use, and limiting GHGs emissions. Instead of burning or dumping the waste, it should be recycled, composted or re-used.

According to this Directive, a target of 50% of the waste from households in the UK, for example, should be recycled, composted or re-used by 2020. The UK government is continuously working to achieve this target. According to the Department for Environment, Food and Rural Affairs (DEFRA)[28], more waste has been re-used and recycled and less landfilled [29]. A new tax was implemented on landfilled waste in 1996; the idea behind this is to reduce the amount of waste sent to landfill sites. It was proposed to encourage waste producers to use more sustainable waste management methods, such as recycling or composting. All sites with an Environmental Permitting Regulations (EPR) permit recovered 64% of their waste in 2014, compared to 39% in 2000, and 59% in 2013, 14% of waste produced by those sites was sent to landfill in 2014, the lowest proportion on record 17% was deposited on land as part of a recovery operation. The landfill allowances for the UK are shown in Table 2.1.

*Table 2.1: Landfill Allowances for the UK*

<b>Maximum Amount (tonnes)</b>			
<b>Area</b>	<b>Target Year Ending in 2010</b>	<b>Target Year Ending in 2013</b>	<b>Target Year Ending in 2020</b>
United Kingdom	13,700,000	9,130,000	6,390,000
England	11,200,000	7,460,000	5,220,000
Scotland	1,320,000	880,000	620,000
Wales	710,000	470,000	330,000
Northern Ireland	470,000	320,000	220,000

The obligation from the EU Landfill Directive is for England to reduce the landfilling of the biodegradable components of food waste to 35% of 1995 by 2020. Failure to meet these targets exposes England to the possibility of non-compliance fines of up to £500,000 per day. This cost will ultimately be borne by local authorities [30]. If these targets are to be realised, significant changes in current food waste management practice are required [31].

The waste hierarchy was first introduced into European waste policy in the European Union's Waste Framework Directive of 1975. In 1989, it was formalised into a hierarchy of management options in the European Commission's Community Strategy for Waste Management[32].

Figure 2.2 shows the five steps that have been implemented by the EU Waste Framework Directive to deal with the waste issue.

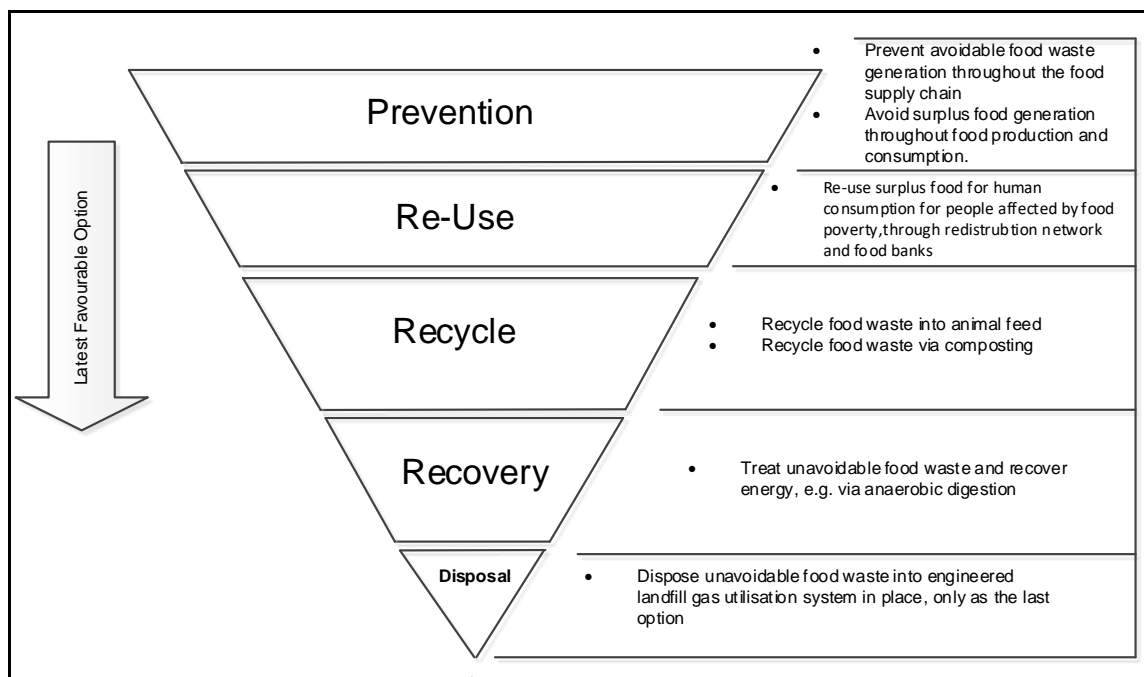


Figure 2.2: Food Waste Hierarchy

## 2.2 Prevention

The first step is prevention and is the ideal outcome of the waste management plan. This step incorporates all the measures that can be taken to reduce the quantity of material that becomes waste. Waste minimisation for food can be achieved by avoiding surplus food generation and better management.

## 2.3 Reuse

The second step is reuse. This step seeks to minimise waste by repairing an item so that it can be reused in the same role. For food, this includes food bank distribution, and could also include cooking and refreezing food that has been defrosted.

## 2.4 Recycle

Recycling materials allow new products to be manufactured from potential waste rather than from new raw materials. Food that is unsuitable for human consumption can be fed to animals. This step also includes composting, as the waste is converted into a fertilizer.

## 2.5 Recovery

The focus of this research is in the recovery step. It is preferred to disposal because it recovers some useful component, such as heat or fuel, and minimises the resulting waste. Applicable methods include waste-to-energy technologies such as anaerobic digestion, gasification, pyrolysis and

incineration. All of which can produce bio-fertilizer, provide heat or generate electricity from the by-products they create.

### ***2.5.1.1 Anaerobic Digestion***

Anaerobic digestion (AD) is a biological process, in which microorganisms known as methanogens decompose organic materials in the absence of oxygen. There are two main types of AD, thermophilic and mesophilic. Thermophilic processes operate at temperatures up to 60°C, whereas mesophilic processes typically operate between 35-40°C. The chosen process depends on the feedstock, with high solid materials tending to favour the higher temperature. This digestion leads to a nearly complete conversion of the organic material into a high energy gas mixture (biogas) consisting mainly of methane (CH<sub>4</sub>) and carbon dioxide (CO<sub>2</sub>), with a smaller percentage of hydrogen sulphide, ammonia and new bacterial biomass [33, 34]. The biogas produced has an energy content of approximately half that of the natural gas. This digestion also occurs in buried municipal waste at landfill sites, the gas produced is then known as landfill gas. The remaining liquid and solid fractions are known as digestate. The liquid fraction can be used as a bio fertilizer; the solid fraction can be composted.

### ***2.5.1.2 Gasification***

Gasification is a thermochemical conversion of solid organic material into a combustible gas by partial oxidation at temperatures typically between 500-1300°C [33] [35]. The gasifying agent can be air, O<sub>2</sub> or steam. The gas

produced is known as syngas, which consists mainly of  $H_2$ ,  $CO$ ,  $CH_4$  and  $CO_2$ . Syngas produced from most biomass wastes usually contains varying amounts of tars and particulate matter. The applications of the syngas are purification level dependent, so these contaminants need to be removed prior to its use. Gas cleaning is important to prevent erosion, corrosion and environmental problems [38, 39]. The presence of tars in the fuel gas is one of the main technical barriers in the biomass and/or biomass waste gasification development.

Robert Gardner obtained the first patent for gasification in 1788 [36], and in 1792 William Murdoch produced gas which was generated from coal to light a room in his house [37]. Coal gas began to be widely used for heating and cooking, and the importance of gasification peaked during World War II due to the reduced availability of oil. The Kyoto Protocol led to renewed interest in gasification. This protocol is an international agreement linked to the United Nations Framework Convention on Climate Change (UNFCCC or FCCC), which commits its Parties by setting internationally binding emission reduction targets, that are directed to protect the earth's atmosphere from gas emissions. Gasification, among other thermochemical waste conversion methods, are believed to have the potential to provide the world with clean and sustainable energy [38, 39].

The feedstock undergoes several chemical reactions, of which some are exothermic and some are endothermic, in order to produce syngas. The main chemical reactions of gasification occurring after the pyrolysis of the wastes are given as followed in Table 2.2 [40, 41]

Table 2.2: Main Chemical reactions of gasification

No	Reaction Name	Reaction Enthalpy $\Delta H^a$
1	$C_nH_mO_k$ partial oxidation	Exothermic
2	Dry reforming	Endothermic
3	Steam reforming	Endothermic
4	Carbon partial oxidation	-110.56kJmol <sup>-1</sup>
5	Water-gas reaction	+131.2kJ mol <sup>-1</sup>
6	Carbon oxidation	-393.65kJ mol <sup>-1</sup>
7	Hydrogasification	-74.87kJ mol <sup>-1</sup>
8	Hydrogen oxidation	-241.09kJ mol <sup>-1</sup>
9	Water-gas shift reaction	-41.18kJ mol <sup>-1</sup>
10	Boudouard reaction	+172.52kJ mol <sup>-1</sup>
11	Methanation	-206.23kJ mol <sup>-1</sup>
12	Carbon monoxide oxidation	-283.01kJ mol <sup>-1</sup>

The temperature is vital to the gasification process, as it will eventually affect the syngas purity. If the heating up is slow, the concentration of volatiles increases rapidly leading to impurity of the produced syngas. If the rate of

heating is high, both pyrolysis and gasification take place simultaneously resulting in low concentration of the volatiles and a cleaner gas is obtained.

Syngas contaminants are summarised in with their effects [42].

*Table 2.3: Syngas contaminant*

<b>Contaminant</b>	<b>Example</b>	<b>Potential Problem</b>
<b>Particles</b>	Ash, char, fluid bed material	Erosion
<b>Alkali Metals</b>	Sodium and potassium	Hot corrosion
<b>Nitrogen Compounds</b>	NH <sub>3</sub> and HCN	Emissions
<b>Tars</b>	Refractive Aromatics	Clogging of filters
<b>Sulphur, Chlorine</b>	H <sub>2</sub> S and HCL	Corrosion, emission

### **2.5.1.3 Pyrolysis**

Pyrolysis is the thermal decomposition of biomass in the absence of oxygen with the objective to obtain as much liquid fuel as possible. It is the first step in the gasification and combustion processes. In combustion, this is followed by total oxidation whereas in gasification only partial oxidation occurs. Pyrolysis differs from gasification because the temperature is not high enough to convert all the organic material to gas, so a liquid fraction (tars and oils) and a char consisting of almost pure carbon is also produced [43, 44].

Pyrolysis can be divided into three subclasses: conventional pyrolysis, fast pyrolysis and flash pyrolysis [45]. The operating parameters for these

processes are summarised by Maschio and others [46] and are given in Table 2.4.

*Table 2.4: Main operating parameters for conventional, fast and flash pyrolysis[46, 47]*

Pyrolysis subclasses → Operating parameters ↓	Conventional Pyrolysis	Fast Pyrolysis	Flash Pyrolysis
Pyrolysis Temp (K)	550-950	850-1250	1050-1300
Heating Rate ( K s <sup>-1</sup> )	0.1-1	10-200	> 1000
Particle Size (mm)	5-50	< 1	< 0.2
Solid Residence Time (s)	450-550	0.5-10	<0.5

#### **2.5.1.4 Incineration**

Incineration involves the combustion of the waste. Combustion is an exothermic reaction between a fuel and a oxidizer to release heat. Combustion of biomass proceeds by two alternative pathways. In the first pathway, which operates at higher temperatures, pyrolysis or thermal decomposition of the biomass provides a mixture of combustible gases. These mix with air and the combustion rapidly spreads in the gas phase. In the second pathway, which dominates at lower temperatures, pyrolysis gives mainly carbonaceous char and a gas mixture containing combustible gases, water and carbon dioxide that is not very flammable. Oxidation of the resulting active char then provides glowing or smouldering combustion[48].

Although theoretically stoichiometric oxygen is demanded because of the inconsistencies in solid fuels, excess air should be supplied to combustion systems. Excess air promotes mixing and turbulence but it decreases the combustion temperature. In low temperature combustion, emissions of odorous and toxic gases may occur[49] and incomplete combustion can result in excessive emissions of particulate matter, fly ash, metal oxides and partially oxidized derivatives, some of which are toxic. The amount of oxygen fed to the system should therefore be carefully controlled. The heat released by the combustion can be used directly, or it can be used to produce electricity[50]. According to the Waste Framework Directive, there is a threshold above which energy efficient municipal waste incinerators can be classified as recovery facilities and below which they continue to be classified as disposal facilities. Incineration can cause serious environmental problems due to carbon dioxide, nitrogen oxides, sulphur dioxide and toxic pollutant such as mercury compound and dioxins.

### 2.5.2 Existing Technologies advantages and limitations.

Technologies	Advantages	Disadvantages
Anaerobic Digestion	<p>Contributes to reducing the greenhouse gases.</p> <p>Feedstock for AD is a renewable source, therefore does not deplete finite fossil fuels.</p> <p>Reduces of soil and water pollution to occur.</p> <p>Convert residues into potentially saleable products.</p>	<p>Potential negative environmental impact.</p> <p>Significant capital and operational costs.</p> <p>Create traffic movement.</p> <p>Required long duration of the microbial reaction which generally in the range of 20-40 days.</p>

Landfill	None	Releases greenhouse and poisonous gases. Pollutes the ground water and produces the chlorofluoro-organic compounds Requires large land area. Unsustainable.
Incineration	Reduces the volume of waste by up to 80–85%.	Releases toxic air emissions containing dioxins and heavy metals.
Pyrolysis and Gasification	Produces hydrogen-rich syngas. Can mitigate emissions of air pollutants by using little or no oxygen. Both gasification and pyrolysis processes work on carbon-based wastes, they are considered appropriate for food wastes	Requires power input. Ash removal required.
Composting	Biological process for converting solid or semisolid organic materials to a stable product.	Creates an offensive odours to the surrounding areas.

## 2.6 Chapter Summary

In this chapter, the food waste management hierarchy and the action taken by EU to overcome this issue is introduced. Further explanation of the current methods is provided with the advantages and disadvantages of each being summarized. Chapter Three will explain about the Electromagnetic Wave Theory

# ELECTROMAGNETIC WAVE THEORY

## 3 : Electromagnetic Radiation

Electromagnetic radiation (EM) is a phenomenon in which energy self-propagates in the form of waves. EM radiation is made up of magnetic and electric fields travelling perpendicular to each other and to the propagation direction. They are classified according to their wavelengths and frequency. All EM waves travel in a vacuum at the speed of light ( $c = 299792458 \text{ ms}^{-1}$ ). EM spectrum can be seen in Figure 3.1

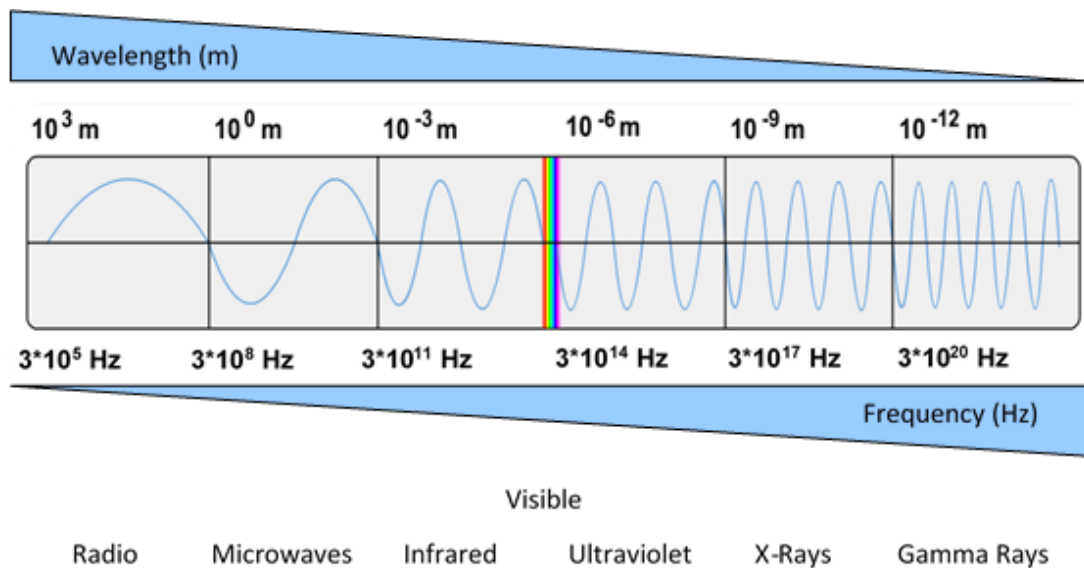


Figure 3.1: EM Wave Classification [51]

### 3.1 Microwaves

Microwaves are a descriptive term used to identify the part of the electromagnetic spectrum, in the range 300 MHz to 300 GHz, with corresponding electrical wavelengths ranging from 1m to 1mm respectively.

EM radiation of the microwave type is used for communications (wireless LAN, MAN, cable TV), remote sensing (radar, radio astronomy), navigation (GPS, Russian GLONASS) and power (microwave oven, microwave chemistry)[52].

Microwaves can be transmitted with low loss using waveguides. Waveguides are hollow metal tubes. Although the cross section of waveguides can be of any shape, the only ones with significant usefulness are rectangular or circular. They are mostly used for frequencies above 300MHz because a waveguide's internal dimensions are directly related to the operation frequency. This means that when the frequency is low (and the wavelength is high), the size of the waveguide is large [53]. Therefore, it becomes impractical and costly to use waveguides at frequencies lower than 300MHz. Table 3.1 shows a list of rectangular waveguide dimensions and their corresponding frequencies [54]. For the work done in this thesis, WG9A (WR340) rectangular waveguides was used because of their practical shape and suitability with the frequency utilised (2.45 GHz).

*Table 3.1: Waveguide Dimensions and their Operating Frequencies*

Std. UK Designation	Std. US Designation	Dimension a (mm)	Dimension b (mm)	Frequency Range (GHz)
WG00	(WR2300)	584	292	0.32 – 0.49
WG0	(WR2100)	533	267	0.35 – 0.53
WG1	(WR1800)	457	229	0.41 – 0.625
WG2	(WR1500)	381	191	0.49 – 0.75
WG3	(WR1150)	292	146	0.64 – 0.96
WG4	(WR975)	248	124	0.75 – 1.12
WG5	(WR770)	196	98	1.96 – 1.45
WG6	(WR650)	165	83	1.12 – 1.70
WG8	(WR430)	109	55	1.70 – 2.60
<b>WG9A</b>	<b>(WR340)</b>	<b>86</b>	<b>43</b>	<b>2.10 – 3.00</b>
WG10	(WR284)	72	34	2.60 – 3.95
WG11a	(WR229)	58	29	3.30 – 4.90
WG12	(WR187)	47	22	3.95 – 5.85

## 3.2 Waveguide Transmission

An EM source, which produces an electrical fluctuation of high frequency between to the wide walls of a rectangular tube, will cause an electron excess on the top wall of the tube and a corresponding deficit in the bottom wall. There is a potential difference between both walls, which is denoted by the vector  $E$  in Figure 3.2

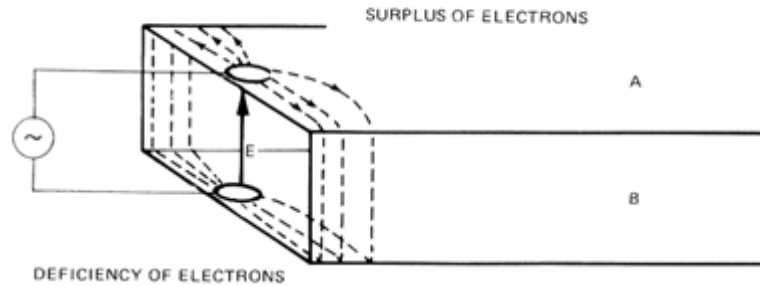


*Figure 3.2: Potential difference in waveguide*

The potential difference between the walls causes electrical currents to flow. This creates magnetic fields trying to circle around the currents. Because of the presence of the metal walls, the magnetic fields cannot completely encircle the currents so they join up. As the oscillator reverses polarity, the vectors created by the currents on the walls themselves generate other currents further along the waveguide by induction, which in turn produces more E and H vectors.

More electric and magnetic fields are created along the waveguide with the continuing alternating current from the microwave source. Figure 3.3 shows how the electrons move and how the electric and magnetic forces move when a microwave source is connected to a waveguide.

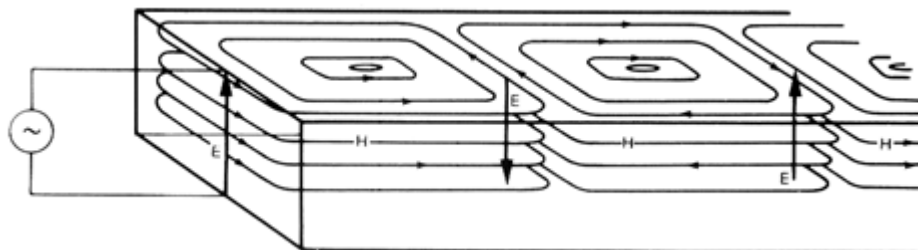


*Figure 3.3: Movement of Electric 'E' and Magnetic 'H' fields inside a waveguide*

These fields propagate inside the waveguide, satisfying Maxwell equations[55], forming regular patterns known as modes. This EM field distribution can be expressed as a superposition of plane waves and is generally termed as transverse electric (TE) modes, transverse magnetic (TM) modes or transverse electromagnetic (TEM) modes. These terms indicate that, in the direction of propagation, the TE modes have no electric field component, TM modes have no magnetic field component, and TEM modes have neither electric nor magnetic field components[56]

The TE signifies that the electric fields are transverse to the direction of propagation and that no longitudinal electric field is present. There is a longitudinal component of magnetic field and for this reason the TE waves are also called H waves. The first index indicates the number of half wave loops across the width of the guide and the second index, the number of half wave loops across the height of the guide. It is advisable to choose the dimensions of a guide in such a way that for a given input signal, only the energy of the dominant mode can be transmitted through the guide. Some typical propagation modes are shown in Figure 3.4.

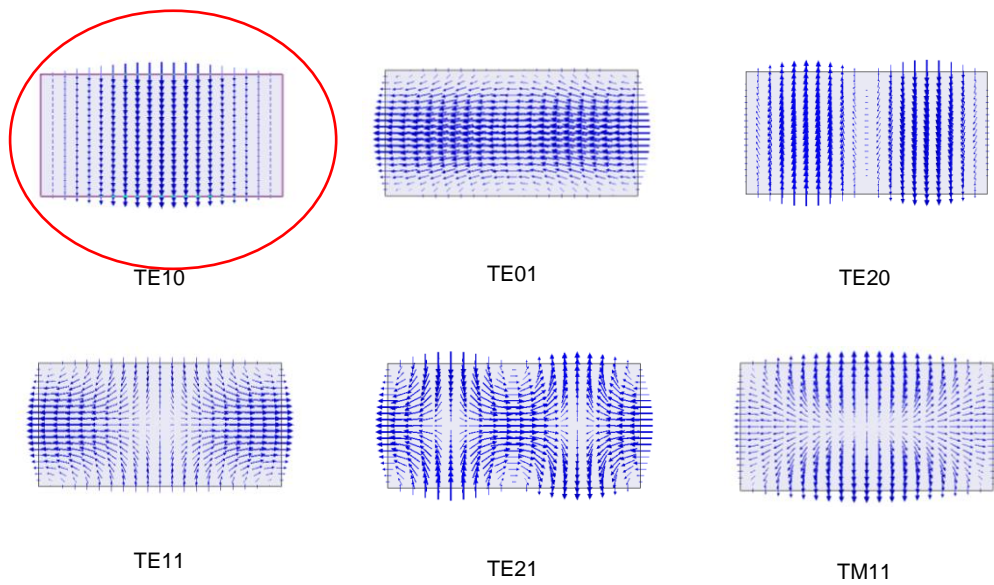


*Figure 3.4: Examples of Transmission Modes in Waveguides*

The electric vectors cancel to produce zero electric field next to the cavity walls and they combine at the centre of the waveguide therefore producing the maximum disturbance. This disturbance is double the amplitude of any single disturbance. Figure 3.5 shows that the distance between full parallel lines is the distance between the two peaks of the electric field when in free space

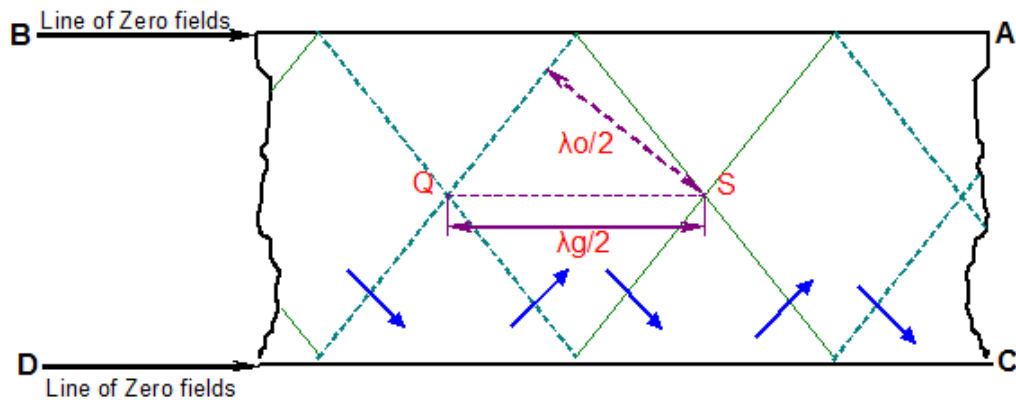


Figure 3.5: Inside a waveguide ( $TE_{10}$ )

The wavelength in free space,  $\lambda_0$ , is defined by equation (3.1) where  $f$  is the frequency (Hz) and  $c$  is the speed of light in a vacuum. .

$$\lambda_0 = \frac{c}{f} \quad (3.1)$$

The distance between a segmented line and a full line is half of a wavelength in free space ( $\lambda_0/2$ ). The distance between two intersections of any two full lines along the centre line (points Q and S for example) is the distance between maximum disturbances and this is called the waveguide wavelength ( $\lambda_g$ ).  $\lambda_g$  is a function of the wavelength in free space and the waveguide dimensions. For the  $TE_{10}$  mode,  $\lambda_g$  is given by equation (3.2).

$$\lambda_g = \frac{\lambda_0}{\sqrt{1 - \left(\frac{\lambda_0}{2a}\right)^2}} \quad (3.2)$$

### 3.2.1 Cut-off Frequency

The cut-off frequency of a waveguide is the lowest frequency for which radiation will propagate. Figure 3.6 show the pattern of the cut off frequency.

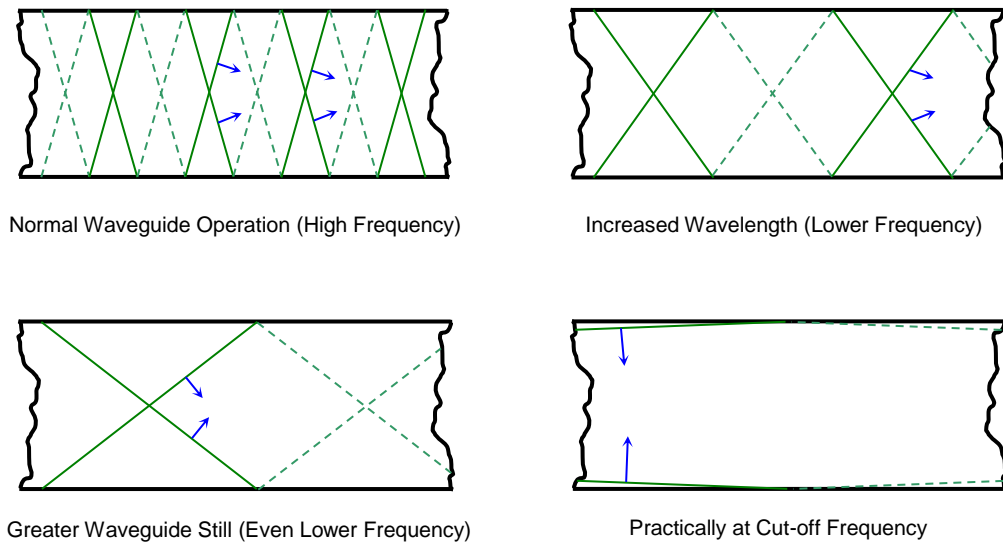


*Figure 3.6: Concept of Cut-off Frequency*

A lower frequency will attenuate rather than propagate. Electromagnetic radiation can be transmitted inside a rectangular waveguide only if the free space wavelength is less than twice the width of the waveguide. The cut-off frequency therefore represents a boundary in the system response at which energy entering the system begins to be attenuated or reflected instead of being transmitted.

For a rectangular waveguide, the cut-off frequency (using the angular frequency  $\omega_c$  rad/sec) for  $TE_{mm}$  modes is given by equation (3.3) [57]

$$\omega_c = c \sqrt{\left(\frac{n\pi}{a}\right)^2 + \left(\frac{m\pi}{b}\right)^2} \quad (3.3)$$

where  $c$  is the speed of light, and  $n$  and  $m$  are the waveguide mode numbers. The lengths of the sides of the waveguide rectangle are denoted by  $a$  (the width) and  $b$  (the height).

The dominant mode in a particular waveguide is the mode having the lowest cut-off frequency. For a rectangular waveguide this is the  $TE_{10}$  mode. Equations (3.4) and (3.5) show the cut-off frequency in a WG9A waveguide for the  $TE_{10}$  mode in terms of both radian per second and hertz.

The dimensions for WG9A are  $0.086\text{m} \times 0.043\text{m}$

$$\omega_c = 3 \times 10^8 \sqrt{\left(\frac{1\pi}{0.086}\right)^2 + \left(\frac{0\pi}{0.043}\right)^2} = 10959044.14 \text{ rad s}^{-1} \quad (3.4)$$

$$f_c = \frac{\omega_c}{2\pi} = 1.74 \text{ GHz} \quad (3.5)$$

### 3.3 Chapter Summary

In this chapter, the fundamentals of electromagnetic wave theory were introduced. Waveguide properties and modes of propagation were detailed. The waveguide used in this research is rectangular and the mode is  $TE_{10}$ . Impedance of transmission lines was explained as was the importance of impedance matching and the utilisation of the tuning systems in microwave applications. Chapter Four will explain about the Atmospheric Microwave Plasma Gasification System.

# Atmospheric Microwave Plasma Gasification

## System

### 4 : Introduction

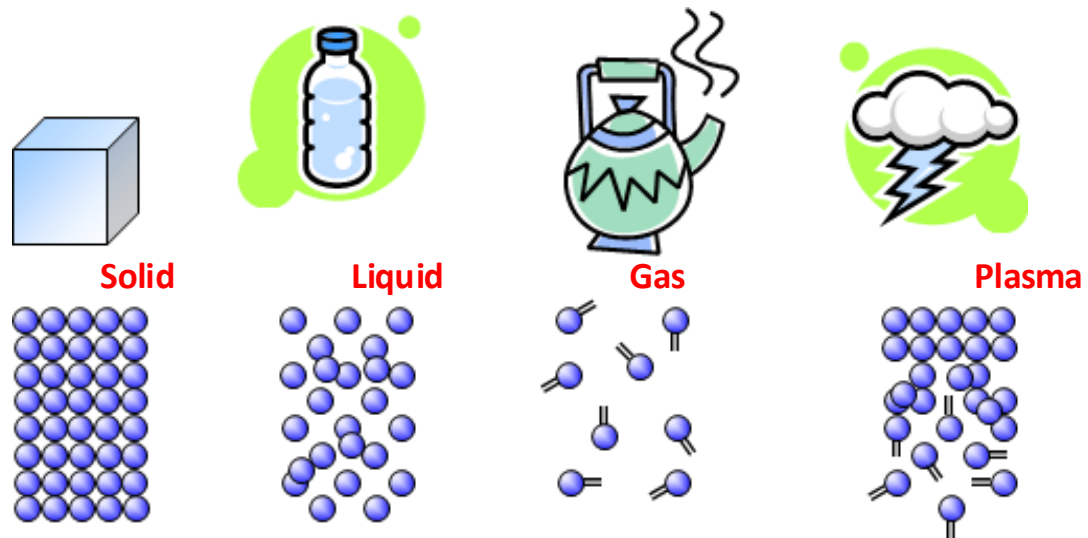


Figure 4.1: States of the matter[58]

Plasma is defined as the fourth state of matter, as represented in Figure 4.1. It differs from gas in that it has been either partially or completely ionized. Plasma can be considered as a “quasi-neutral system” of a large number of charged particles which exhibit collective behaviour. [59, 60].

In high pressure or thermal plasmas all the electrons, ions, atoms and molecules are in thermal equilibrium. Atmospheric pressure or non-thermal plasmas are those for which the electrons are at a high temperature compared to the temperature of the ions, atoms and molecules. The free electrons can cause the molecules to split apart producing reactive fragments or free radicals but not all the molecules will be dissociated.

Plasmas have two main characteristics, temperature and energy density, which are very important for practical applications. The temperatures and energy densities produced by plasma are greater than those produced by ordinary chemical mechanisms. Plasmas can therefore be used for specific applications that cannot be achieved through more conventional methods [61].

## 4.1 Plasma Excitation Sources

Plasma is usually excited and sustained by providing an electromagnetic field. This can be achieved in different ways but includes: direct current (DC), alternating current (AC), radio frequencies and microwaves [62]. AC and DC plasmas require electrodes and high power to ensure electrons jump from the cathode surface to the anode, while for microwave plasma, the electric field can ionise a gas without an electrode [63, 64]. The advantages of microwave generate plasma over a typical DC generate plasma are: [60].

- The electrode erosion is less significant as the nozzle stays relatively cold since the plasma operates at the tip of the nozzle [65].
- The plasma jet is more stable as there is less vapour contamination from the nozzle [65].

## 4.2 Gas Interaction with Microwaves

The electrons in a plasma system are the main element that controls the energy transfer from the external electric field to the discharge. However, both ions and electrons interact with the applied external electric field and are accelerated by absorbing energy from it. Electrons are the lightest particles in

the plasma, so they are the easiest to accelerate and absorb the majority of the microwave energy. A higher microwave field will then result in more electrons and atoms accelerating and a higher concentration of plasma.

Particles in plasma are in continuous motion and this results in collisions between the particles. The collisions can either be elastic or inelastic. Elastic collisions are those between the electrons and the heavier particles that do not result in an excitation. Inelastic collisions are the collisions that cause dissociation or ionization [66].

Argon has been used in this research as the plasma gas as it is relatively cheap. It has a very low elastic energy transfer compared to its inelastic energy transfer [67], this makes it a good source for plasma creation. Helium is another noble gas that is also suitable for plasma discharge applications. Helium can be considered better than argon for plasma creation [68-70] because it has a greater thermal conductivity (He  $1.520 \text{ mW cm}^{-1} \text{ K}^{-1}$  versus Ar  $0.1772 \text{ mW cm}^{-1} \text{ K}^{-1}$ ) and a lower mass. The greater thermal conductivity accelerates the rate of ionisation. It is however much more expensive than argon and is therefore unsuitable for scale-up.

The flow rate of the plasma gas also effects its interaction with microwaves [71]. The increase of gas flow rate provides more gas particles at a given period of time. However, the residence time in the plasma is reduced, which results in a lower plasma density for a given microwave power.

### 4.3 Key Microwave Plasma Gasification Parameters

Microwave plasma syngas production depends on the microwave power level and the gas flow rate. This also includes the reflected power, which should be at a minimum level to maximise the delivered power to the gas-microwave interaction region.

The gas flow rate and the power level actually determine the plasma temperature. Other key parameters of the gasification process are the pressure inside the gasification chamber and the type and properties of the sample used. All of these parameters are studied in this project and can be listed as follows:

- The effects of the pressure inside the gasification chamber,
- The effects of the sample's moisture,
- The effects of argon flow rate as a part of plasma temperature parameter,
- The effects of power source level as a part of plasma temperature parameter,

There are a number of papers reporting microwave plasma gasification technologies [72-75]. These papers study the gasification of coal and biomass for syngas production rather than for waste applications.

This chapter describes the design of the microwave plasma cavity that has been used for this research. The plasma cavity is basically a short-circuited rectangular waveguide. It contains a nozzle through which the plasma gas is passed. The gas encounters a large electric field when it exits the nozzle and

this causes ionization to occur. The short circuit creates a standing wave, and the nozzle is positioned so that it coincides with the highest possible field for any given power. The tapered shape of the nozzle also enhances the field. To create self-striking plasma, the electric field had to be increased further again.

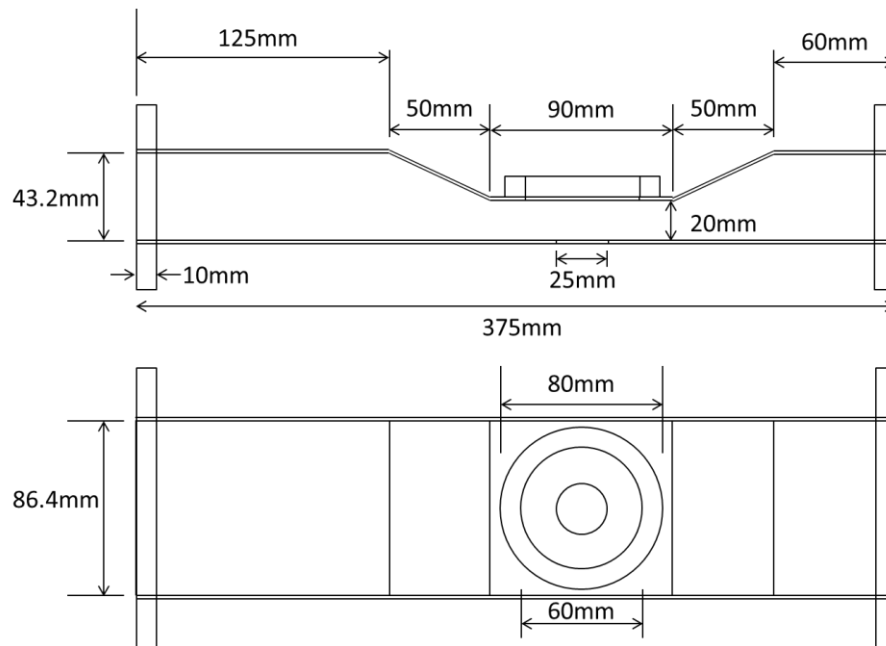


Figure 4.2: Plasma Cavity Design

This can be done by increasing the applied power, but doubling the electric field requires the power to be quadrupled as the magnetic field would also be doubled. A more effective method is to reduce the waveguide's 'b' dimension close to the nozzle. This change must be gradual to avoid unwanted reflections. A single-sided taper design is shown in Figure 4.2, but the cavity used for the majority of this work used the two-sided taper design shown in Figure 4.3. and Figure 4.4. The principle is the same but using a two-sided design proved simpler to construct.

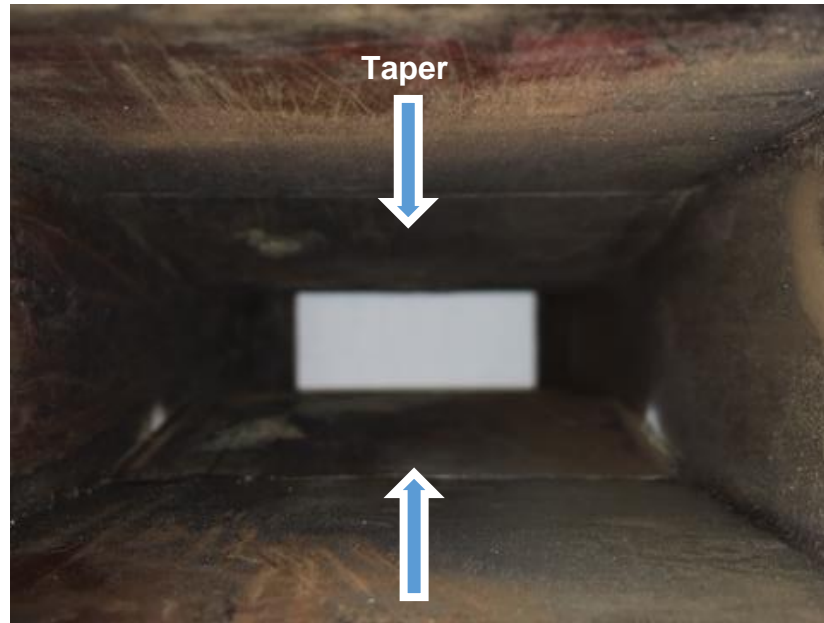


Figure 4.3: Two-sided taper design

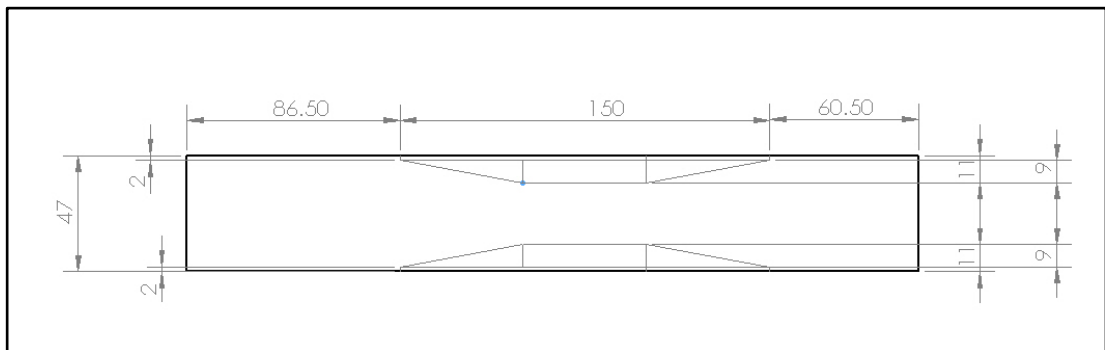
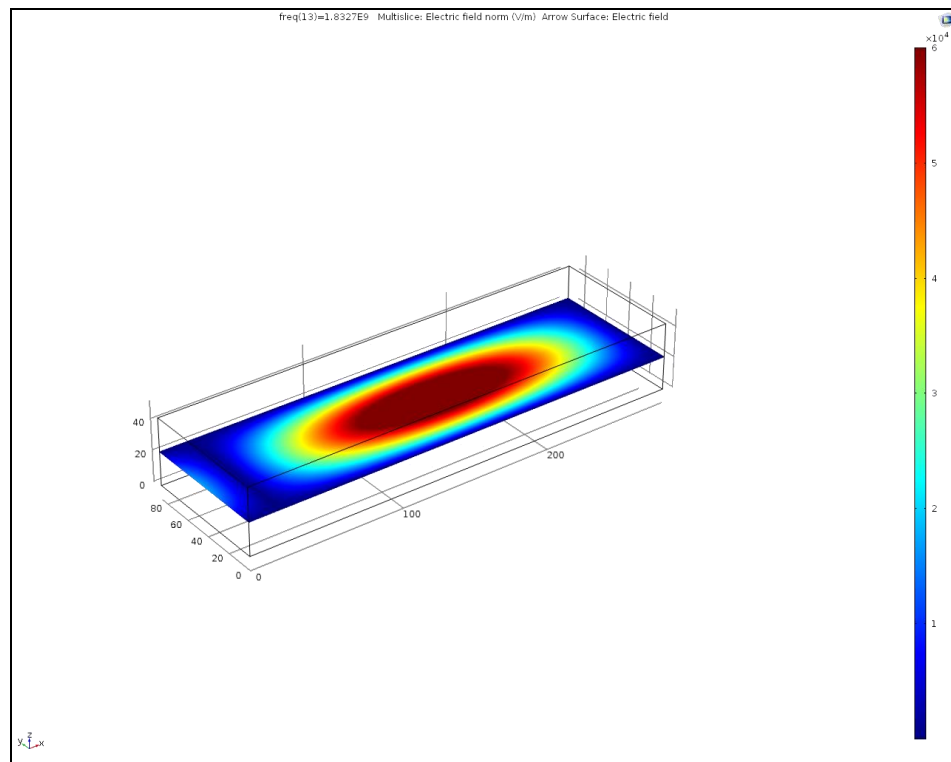


Figure 4.4: Double sided taper design

## 4.4 Microwave Plasma Cavity Modelling

Waveguide modelling was performed using the COMSOL Multiphysics® RF. This software uses finite elements to simulate the electromagnetic fields within the plasma reactor waveguide. COMSOL Multiphysics contains ready-made, built-in interfaces for modelling electromagnetic wave propagation and resonant behaviour and field distributions.

For this research the  $TE_{101}$  mode has been chosen because of the stronger electric field in the centre of the waveguide, this can be observed from the simulation results in Figure 4.5, which shows how the maximum E-field occurs at the centre of the cavity.



*Figure 4.5: E- field simulation for the  $TE_{101}$  mode in WG9A waveguide*

The E-field magnitude at the centre of the waveguide length is shown in Figure 4.6.

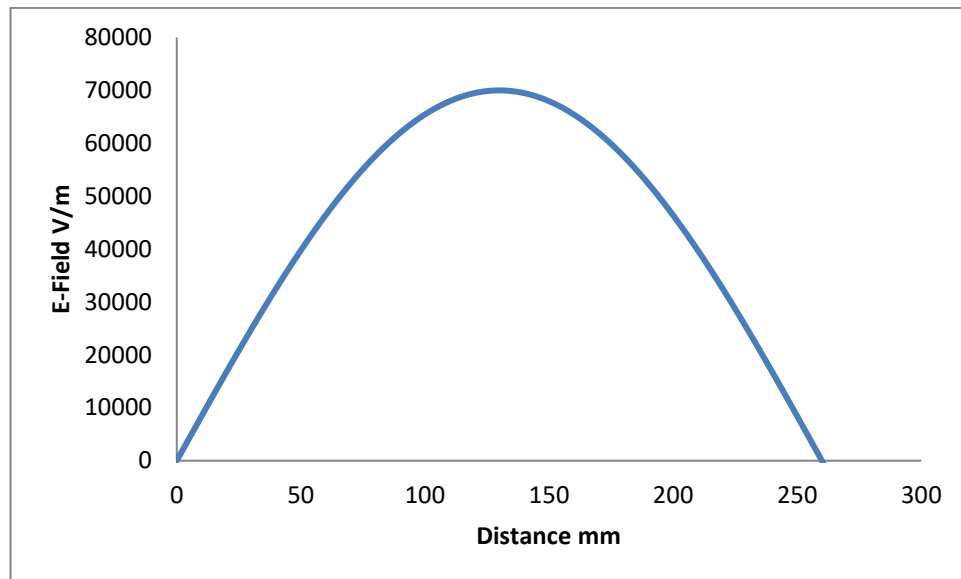


Figure 4.6: E- field magnitude for the  $TE_{101}$  mode in WG9A waveguide

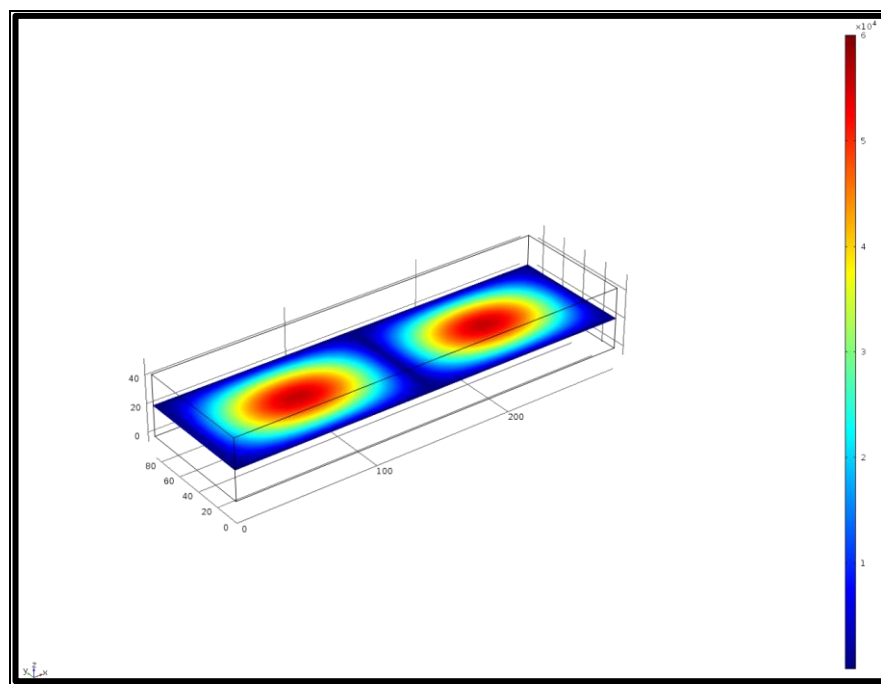


Figure 4.7: E- Field simulation for the  $TE_{102}$  mode in WG9A waveguide

Figure 4.7 shows the simulation for  $TE_{102}$  but the same result is achieved if a travelling wave is reflected from one end, with the maximum electric field occurring at a distance of  $\lambda_g/4$  as well as at  $3\lambda_g/4$  etc, as shown in Figure 4.8.

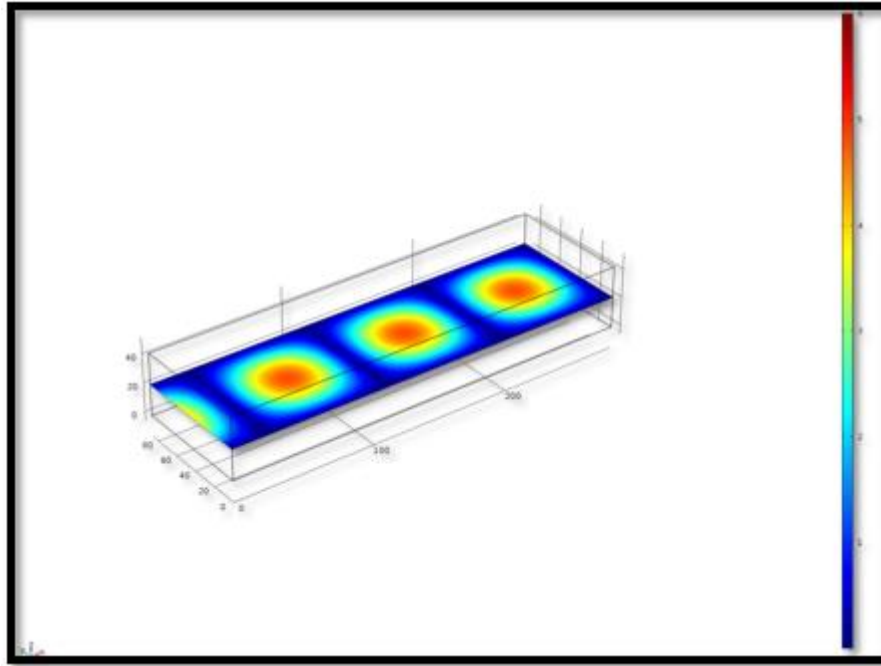


Figure 4.8: Travelling wave with short circuit at far end

The magnetron used for this project generates a frequency in the range  $2.45\text{GHz} \pm 10\text{MHz}$ . The waveguide wavelength at this frequency, assuming the waves are travelling at the speed of light  $c$ , is shown in equation (4.1).

$$\lambda_g = \frac{c}{\sqrt{1 - \left( \frac{c}{2(86 \times 10^{-3})(2.45 \times 10^9 \pm 10 \times 10^6)} \right)^2}} = (174 \pm 1) \text{ mm} \quad (4.1)$$

A hole is cut out in the plasma cavity to allow the plasma jet to escape. Figure 4.9 shows the E-field simulation of the waveguide from the side when the nozzle is inserted above the hole.

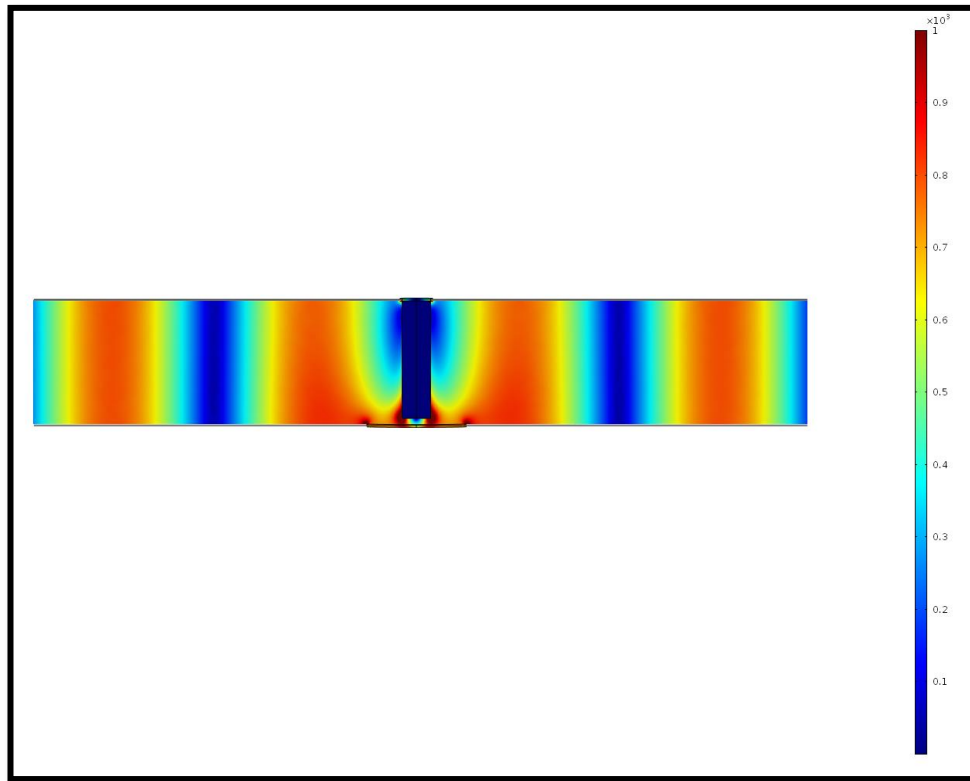


Figure 4.9: Simulation of waveguide with the nozzle

### 4.5 Microwave plasma gasification system

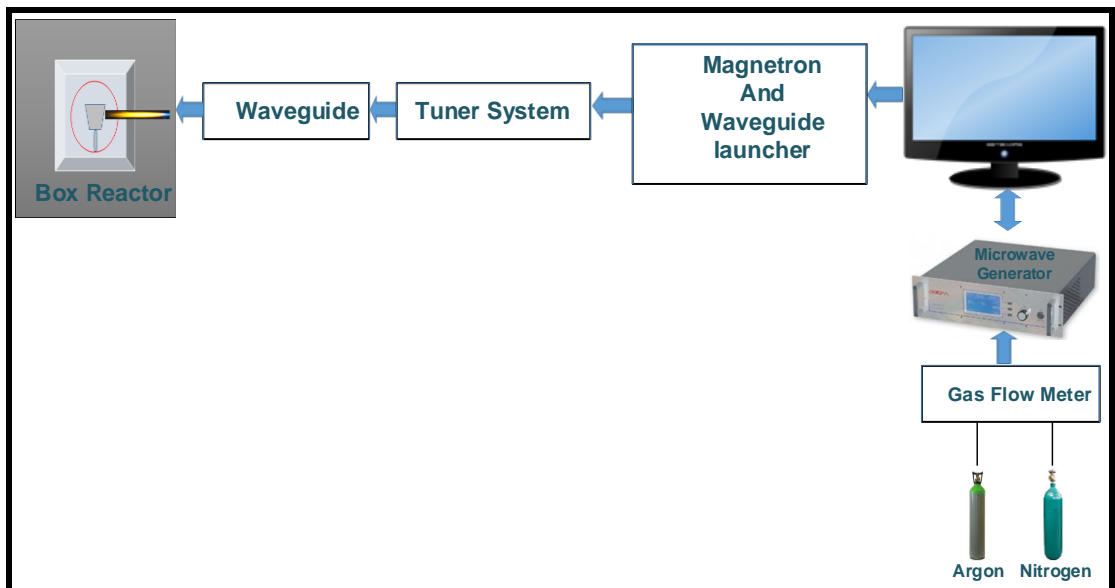
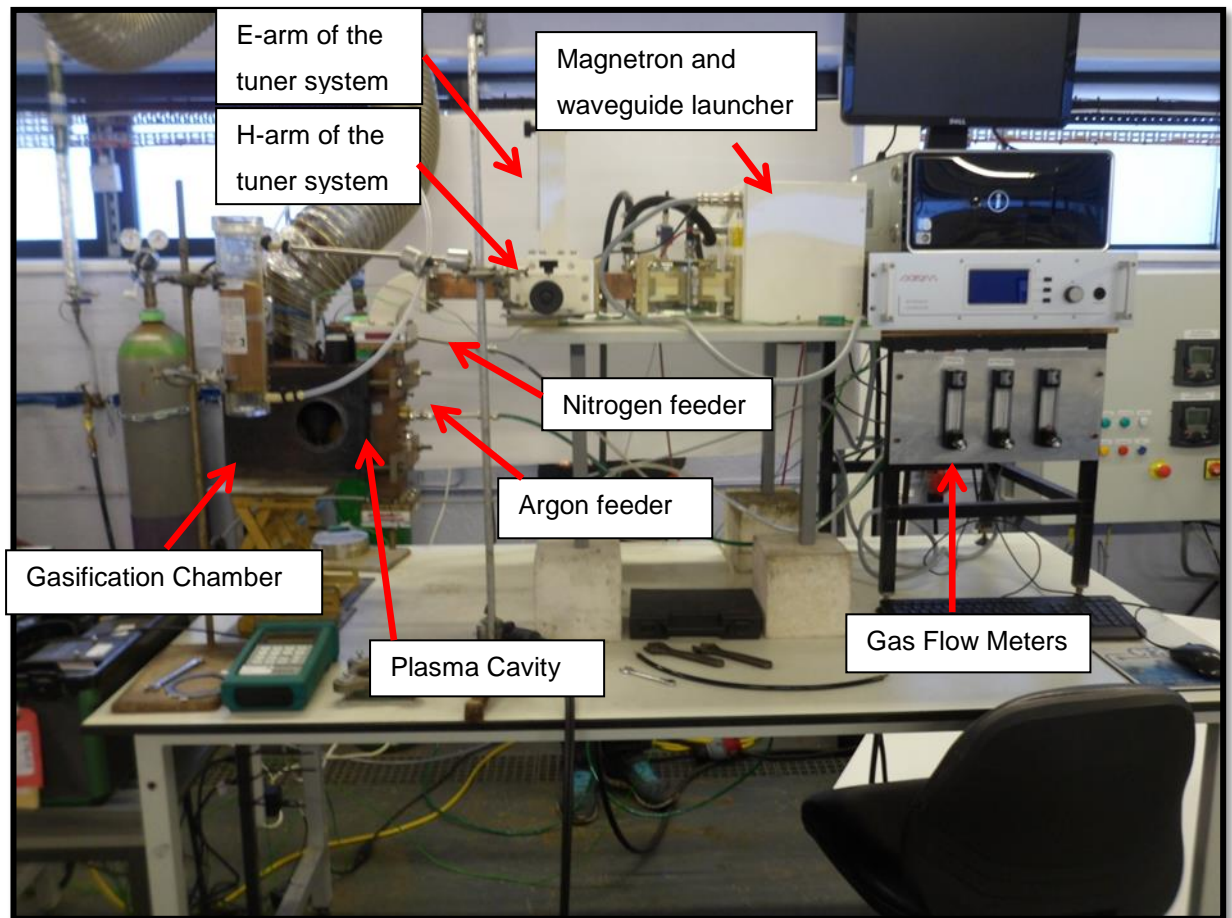


Figure 4.10: Block diagram of the experimental set-up



*Figure 4.11: Microwave plasma gasification system.*

Figure 4.10 shows the block diagram of the experimental set-up and Figure 4.11 demonstrated the lab based microwave generated plasma gasifier system. The magnetron is connected to an isolator. This is a circulator with a built-in matched load. The circulator uses ferrite discs in a constant magnetic field to direct the input power towards the plasma cavity, and the reflected power into the matched load, where it is dissipated to protect the magnetron. The plasma cavity is connect to the isolator via an EH tuner. The plasma cavity was placed in an upright position on the side of the gasifier as shown in Figure 4.12. This was done to maximise the power and minimise the gas use while maintaining stability. If the plasma jet flows downward, then the hot gases

produced will rise and can enter the cavity causing instabilities. More plasma gas can reduce this effect but this is not ideal. The lowest gas use, which also results in the highest temperature, is to have the plasma jet upwards, but then the cavity is more susceptible to instabilities due to falling solids and condensate. The side approach was therefore seen as the best compromise.

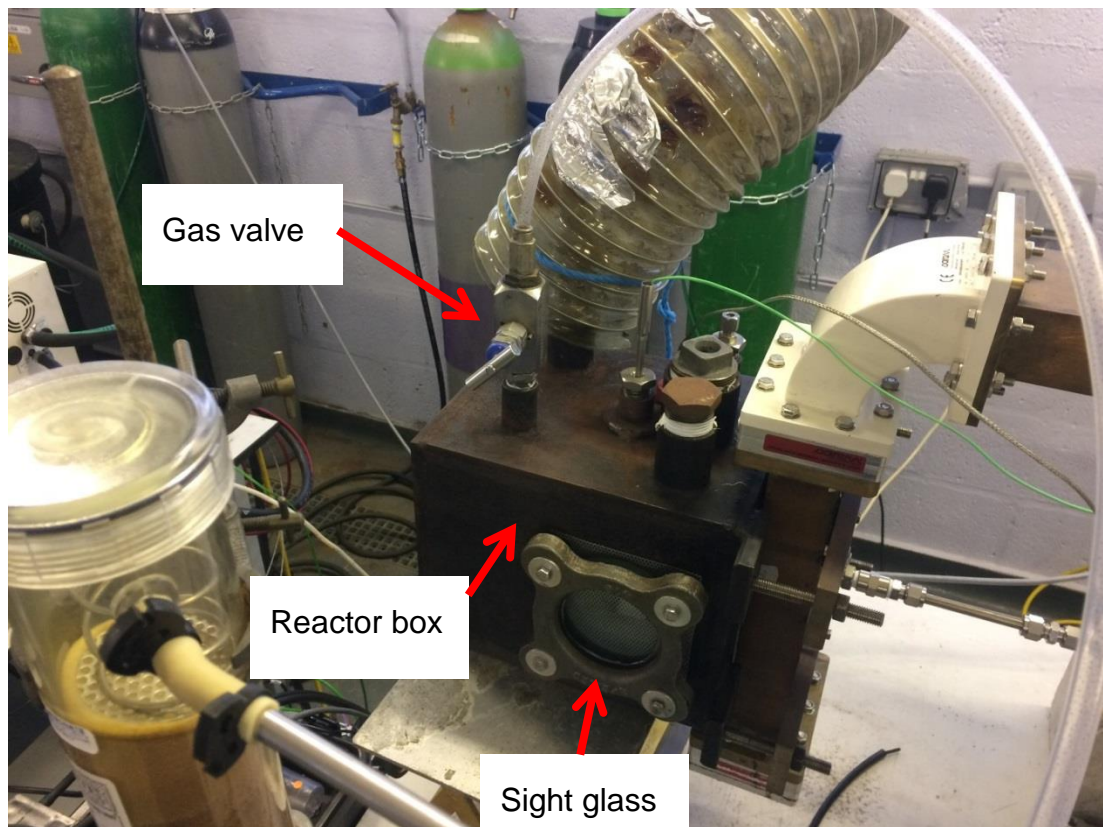


*Figure 4.12: Gasification reactor and plasma cavity.*

The EH tuner was manually controlled for impedance matching to maximize the amount of power entering the cavity. The microwave power supply, model number GMP60KIP56T400FST3IR, was manufactured by Sairem, and can deliver 6 kW at 2.45GHz.

## 4.6 Gasification Reactor

This gasification reactor is where the feedstock is placed for syngas production. The reactor was sealed to maintain the pressure inside and to prevent the ingress of oxygen. The pressure could be controlled manually, but there was also a pressure safety valve set at 300mbar. Syngas produced from the gasification process is exhausted from the system for analysis through gas exhaust pipe. The interaction between the plasma and the feedstock could be observed through the sight glass on the front side of the reactor.

## 4.7 Gas Feed Control

Argon was used as the main plasma gas and nitrogen was used to purge the gasifier of oxygen, to maintain the pressure and to keep steam, smoke and other particles out of the plasma cavity. The reason these gasses was chosen because it were cheap. The flow rates were manually controlled. Typical values were 1.5 L/min for argon and 5L/min for nitrogen. This values was selected based on several trials with different flow rates has been carried out in term of optimise the best flow rate for this research. The actual flow rates depended on the power level and the nozzle diameter. In terms of health and safety of argon and nitrogen are asphyxiants. In higher levels they can cause nausea, vomiting, unconsciousness, coma and death. No occupational exposure limits have been established [76].

## 4.8 Self-striking plasma

When the power is initially applied the EH tuner must be set in the correct tuning position for the plasma to self-strike. Once it is established, the impedance presented by the plasma cavity changes due to the interaction between the plasma and the microwaves. The tuner must then be readjusted to maximise the forward power under the new conditions.

## 4.9 Temperature Thermocouples

The temperature of the plasma was measured using a K-type thermocouple like that shown in Figure 4.13 [77]. These is able to measure temperatures in the range 0-1200°C. Thermocouples measuring temperatures inside the gasifier were placed in thermopockets. This avoids interference problems that can occur with the thermocouples in a microwave fields. Two thermocouple sensors were used, a magnetic thermocouple was attached to the reactor to monitor the external wall temperature, and the second thermocouple sensor was placed inside a thermopocket that was positioned directly above the crucible that held the food sample.

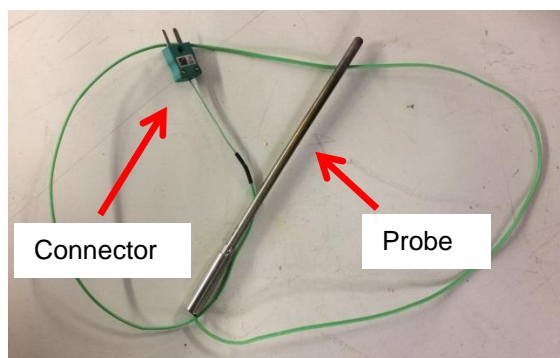


*Figure 4.13: K-type thermocouple*

The thermocouples were connected to a National Instruments NI 9211 cDAQ module and the temperatures were recorded using LabVIEW.

A Flir infra-red camera model (T420) was also used to monitor the external temperature profile of the gasifier and plasma cavity. Images from this camera are shown in Figure 4.14.

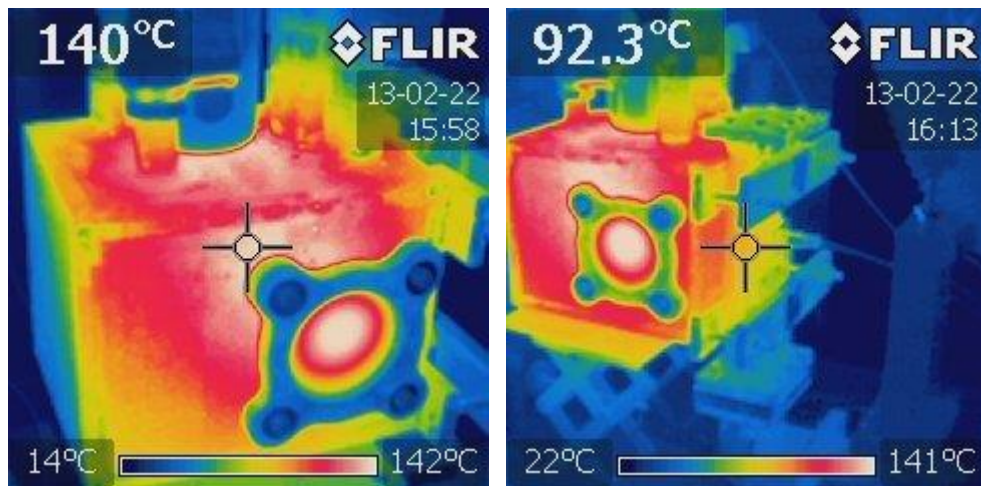


Figure 4.14: Infra-red images of the gasifier and plasma cavity

#### 4.9.1.1 cDAQ Chassis



Figure 4.15 : Cdaq 9172 and Cseries compatible modules (ni.com)

Figure 4.15 shows the cDAQ 9172, which is used to control the gasification system. This chassis contains eight module slots and is compatible with all of

the available DAQs modules from NI. Four NI DAQs were used in the control system as shown in Figure 4.16 (a) and (b):



Figure 4.16: (a) NI units for the power control (b) NI units for the temperature control

- **NI 9401** [78] is a 8-channel, 100ns bidirectional digital module. It was used for the control Input/output power on the Sairem unit.
- **NI 9211** [79] is a thermocouple input module. It was used for temperature measurement (feedback parameter).
- **NI 9263** [80] is a 16-channel, 100ks/s/ch simultaneous analogue output module. It was used to control the output power on the Sairem unit.
- **NI 9205** [81] is a 32 single-ended or 16 differential analogue inputs, 250kS/s. It was used to log the reflected power from the Sairem unit.

## 4.10 Power Control

The power generator provides the magnetron with the desired anode current and the necessary high voltage. The anode current is used to control the output power. The reflected power is measured using a diode detector, which produces a voltage in response. The power generator can be operated both manually or through a control program (i.e. LabVIEW).

## 4.11 Quartz Window

The role of the microwave quartz window is to transfer the microwave energy between two media without inducing any reflected power. The window allows the separation of different environments at pressure close to atmospheric; in addition, the quartz window can be used as a 'light barrier', i.e. hides the light emitted by plasma that could trigger off the arc detector installed in some microwave generators.

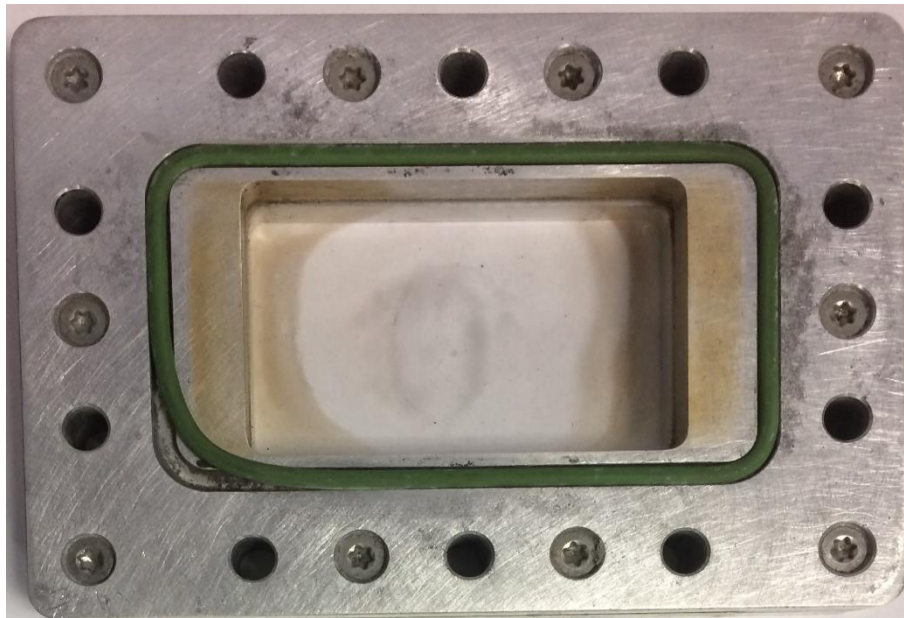


*Figure 4.17: Microwave Window*

## 4.12 Nozzle

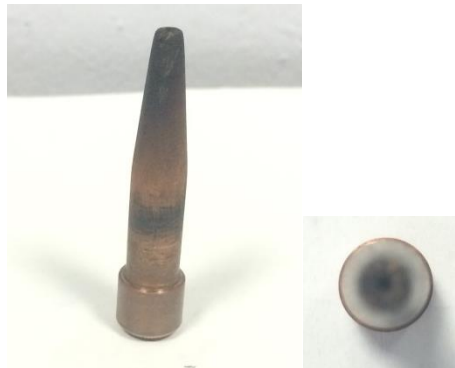


*Figure 4.18: Nozzle overview*

Figure 4.18 show a copper nozzle that was used for this project. Numerous materials, including alumina, have been used to construct nozzles of several designs, but the copper nozzle, shown in Figure 4.18, gave very good results and the best longevity. The nozzle shape is important as it plays a major part in determining the electric field intensity. If the angle of the nozzle is too shallow then the field will be too weak, if it is too acute, the nozzle walls will be thinner and its lifetime will suffer. The diameter of the nozzle aperture is dependent upon the application and varies between 0.3 and 2.0 mm. If the hole is too small for a given power and gas flow rate, then the end of the nozzle is vaporised. The gas supply is fed into the opposite end and a locking nut is used to provide a good electrical connection to the waveguide that is also gas tight. This prevents sparks between the threads when the microwaves are turned on, which causes damage and wastes energy [60].

### 4.13 Quintox Gas Analyser Sensor

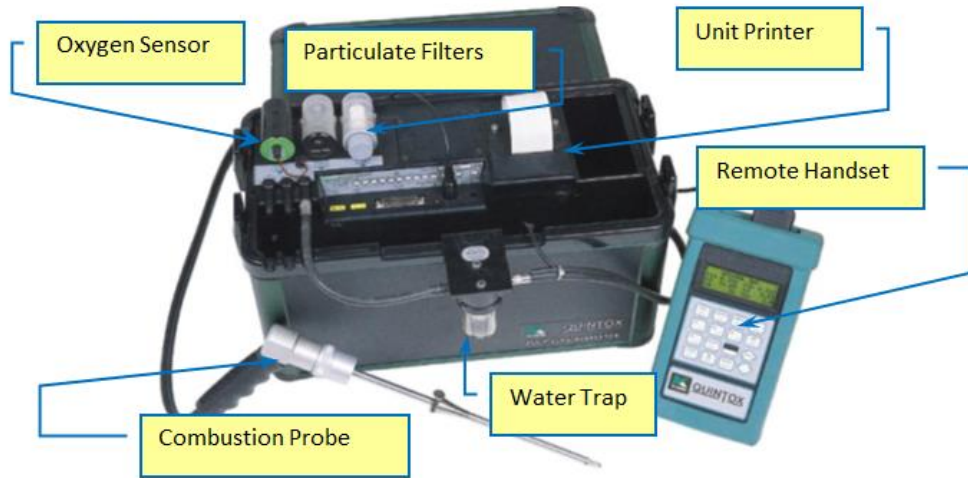


Figure 4.19: Quintox 9106 Gas Analyser

The syngas production rate was monitored using a Quintox gas analyser. This can measure CO, CO<sub>2</sub> and O<sub>2</sub> but not H<sub>2</sub>. The specifications of the gas sensor are shown in Table 4.1. The unit also includes a particulate trap and a water vapour condenser.

Table 4.1: Gas sensor specification.

Gas Measurement	Resolution	Accuracy	Range
Oxygen (O <sub>2</sub> )	0.1%	-0.1% to +0.2%	0-25%
Carbon Monoxide (CO)	0.01%	±5% of reading from 0.1 to 10%	0-10%
Carbon Dioxide (CO <sub>2</sub> )* <sup>2</sup>	0.1%	±1%	0-100%

The unit can measure the gases, and transfer them to a PC via an RS232 serial port every 10 seconds. Interfacing with the PC was done using LabVIEW. The data consists of 33 data items either in binary or as a comma separated value (CSV) output. A list of these data items is given in Table 4.2[82].

*Table 4.2: Parameters Outputted by Quintox 9106*

Time	Date	Instability	Battery %	Sensor	Ambient	Pressure
Fuel	K1g	K1n	K2	K3	K4	O <sub>2</sub> Ref.
Nett Temp.	Flue Temp.	Inlet Temp.	O <sub>2</sub> Reading	Excess Air	CO Reading	
Efficiency	Losses	Dry Loss	Wet Loss	CO Loss	NO	NO <sub>2</sub>
NO <sub>x</sub>	SO <sub>2</sub>	H2xc	Aux1	CO <sub>2</sub>		

## 4.14 Health and Safety for CO

Carbon Monoxide is a toxic to human in a concentration of above 35ppm. It combine with haemoglobin to produce carboxyhaemoglobin (COHb)[83], which reduces the ability of blood transport oxygen from the lungs. Small amounts of COHb lead to tiredness and dizziness. Increased oxygen deprivation inside blood is proportional to the amount of COHb formed [84].

## 4.15 Chapter Summary

Plasma theory was introduced in this chapter as it is used for the pyrolysis/gasification process. The key microwave plasma gasification parameters have also been discussed. These parameters are gas type, microwave power and reflected power, plasma gas flow rate, and the pressure inside the gasification chamber. These parameters are studied further in the Chapters 5 and 6. Chapter Five will explain about the experimental methodology.

## EXPERIMENTAL METHODOLOGY

### 5 : Introduction

In this Chapter, details of the experimental setup and procedures, operating conditions and parameters, analytical techniques and other resources used are presented and described.

#### 5.1 Sample preparation

Food waste was collected from a Byron Hamburger restaurant in Liverpool, UK. The food waste consisted of leftover food from customer plates and food that has been thrown out by the chefs. A typical sample is shown in Figure 5.1



*Figure 5.1: Waste sample*

The food waste items were separated into two different categories. The first category is waste of mixed food which contains a combination of all the foods served, such as burger bun, raw onion, burger meat, fries, lettuce, tomato, bacon and chicken. The second category is paper waste which contains the napkins and grease-proof paper from the customers' plate. Due to the size of material relative to the samples required per test, each category was ground to a uniform consistency by using a blender to produce a homogenous mixture are shown in Figure 5.2. After the grinding process, 10g samples were accurately weighed, placed into a small plastic bag and stored in a freezer. This mass was chosen based on the density of the material and the size of the plasma jet. The reactor crucible was design to sit in the jet, and was only large enough to accommodate this sample size. The paper waste samples were compacted to prevent them falling from crucible during the test.

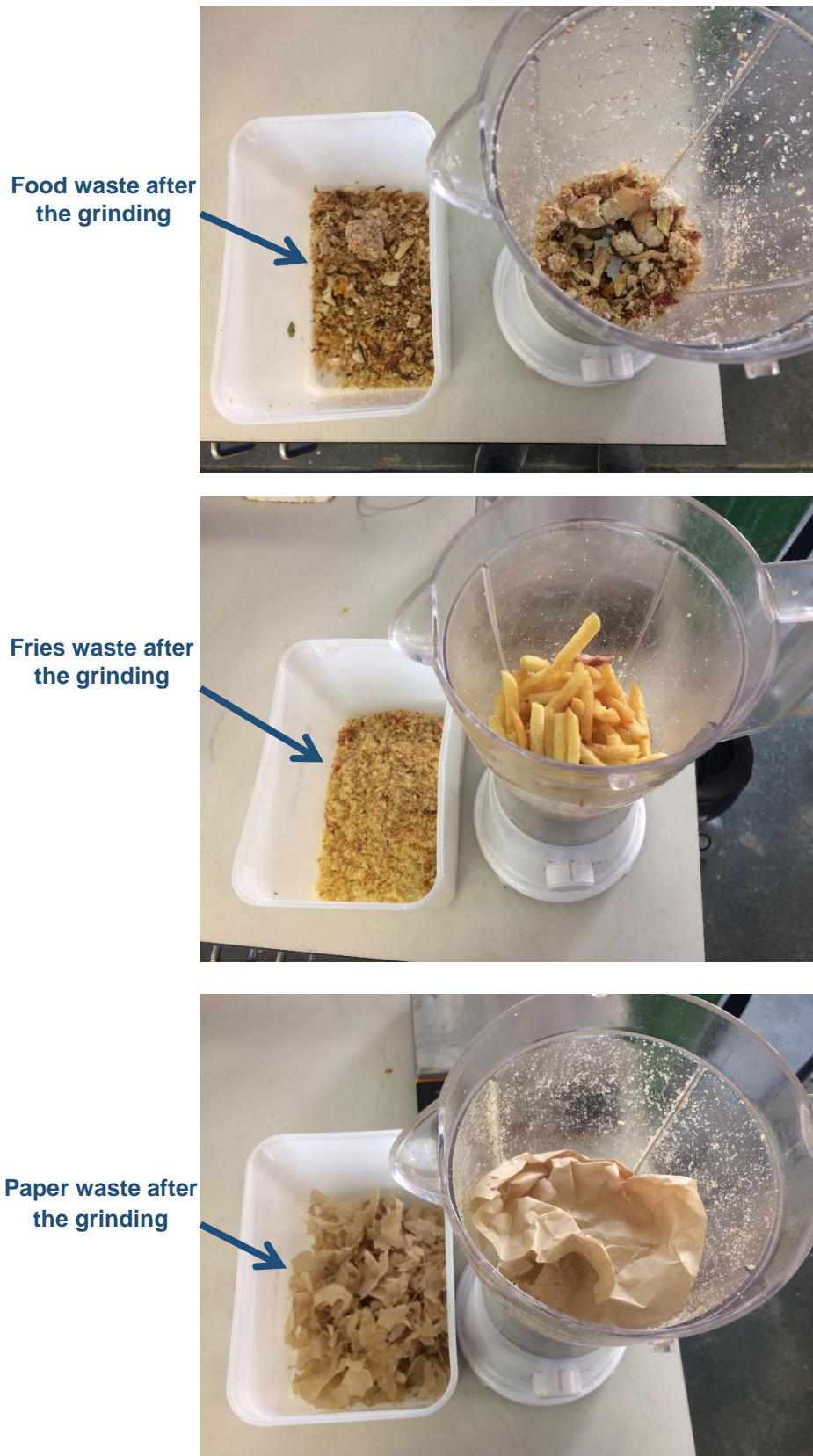


*Figure 5.2: Sample after grinding process.*

## 5.2 Samples Properties Determination

The moisture content of the samples could be found by drying in the laboratory oven at 105°C, as shown in Figure 5.3. Each 10g sample was placed inside a small crucible and weighed. The samples were typically left for 30 min before being reweighed. This process was repeated until the mass was constant. The difference between the final mass and the initial mass was recorded as lost water. Gasification tests were conducted on both dried samples, as well as samples with their original moisture content.



*Figure 5.3: Samples inside drying Oven*

## 5.3 Food Waste Analysis

The chemical composition and calorific properties of waste samples from the Byron Hamburger restaurant were analysed by an external laboratory. The results are presented in Chapter 7. The analysis consists of the following tests:

1. **Total Moisture:** This is the quantity of water in the material, which is expressed as a percentage of the material's mass. The analysis sample is dried at  $(105 \pm 2)$  °C until the mass is constant according to BSEN 14774(3). The moisture content of a sample can be calculated for the mass change during drying according to equation (5.1) [85]

$$\text{Moisture Content} = \frac{\text{original mass} - \text{oven dry mass}}{\text{original mass}} \quad (5.1)$$

2. **Ash content:** Ash is the inorganic component in the waste. The ash content is determined from the residual mass after being heated in air at  $(550 \pm 10)$  °C, according to BSEN 14775. This content is important as it affects the behaviour of gasification and combustion under high temperatures. Melted ash may cause problems in gasification reactors. The ash content can be calculated according to the equation (5.2) [53]

$$\text{Ash content} = \frac{\text{mass of ash} \times 100}{\text{mass of sample}} \times \frac{100}{100 - \text{moisture content}} \quad (5.2)$$

3. **Volatile matter content:** The volatile matter content is defined as the loss of mass when the waste is heated at  $(900 \pm 10)$  °C, after deducting the moisture constant.

$$\text{Volatile matter} = \left[ \frac{(\text{mass of sample} - \text{mass after heating}) \times 100}{\text{mass of sample}} - \text{moisture content} \right] \times \frac{100}{100 - \text{moisture content}} \quad (5.3)$$

4. **Elemental composition:** The carbon, hydrogen, oxygen, sulphur and chlorine can be found by burning a sample in oxygen and analysing gaseous products of combustion .According to BSEN 15104 and BSEN 15289.
5. **Calorific value or heating value:** A sample is burned in high pressure oxygen in a bomb calorimeter[86, 87].
  - The Gross Calorific Value, also known as the higher heating value (HHV) includes the total amount of heat energy in the waste including the energy contained in the water vapour in the exhaust gases.
  - The Net Calorific Value, also known as the lower heating value (LHV), this does not include the energy in the water vapour, as this usually escapes with the exhaust gases.

## 5.4 Microwave-induced plasma gasifier

The experimental microwave plasma gasifier, shown in Figure 5.4, was constructed as a welded steel box (250mm×200mm×200mm). It was insulated with 15mm thick refractory lining (Thermal Ceramic Kaowool 1600). A stainless steel crucible was fitted inside the reactor to hold the test material. The position and height of the crucible could be adjusted to optimize the interaction with the microwave plasma jet. Thermocouples were placed inside and outside the gasifier to monitor the temperature profiles.



*Figure 5.4: Microwave plasma gasifier*

The internal thermocouple was placed directly above the crucible to measure the temperature throughout the experiment. Both temperature profiles were recorded using a LabVIEW program. The stand for the crucible was modified so that it could be accurately positioned relative to the microwave plasma jet. A sight glass with a diameter of 100mm was installed on the side of the box reactor. This both enable the interaction with the plasma to be observed and also provided access to the stainless steel crucible. A perforated stainless steel sheet with 2mm diameter holes, an open area percentage of 47% and a 0.55mm thickness was used in between the box and the glass to reduced microwave leakage below the range of the microwave leakage detector manufactured by SAIREM, which is shown in Figure 5.5.

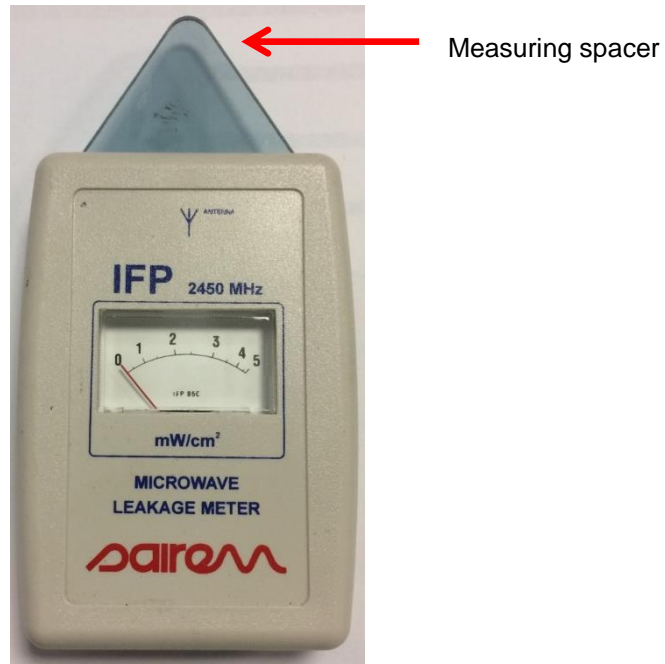


*Figure 5.5: Microwave leakage detector*

## 5.5 System Experimentation and Parameters

The experiments were designed to understand the behaviour of the gasification process in relation to the system's various parameters such as power level, argon and nitrogen flow rates and pressure. The benefit of these experiments was to determine the system parameters to optimise temperature and stability.

### 5.5.1 Power

A 6kW microwave generator (SAIREM GMP60KIP56T400FST3IR) [88] was used to power the plasma. The forward power was adjustable from 10% to 100% in 10W steps using LabView. This software monitored the reflected power from the diode detector. Both of these powers were calibrated after interfacing with the cDAQ. The output was calibrated using a water-cooled

matched load by measuring the temperature difference of the water into and out of the load. The temperature difference can then be compared to the specific heat capacity of water. The reflected power calibration was performed by shorting the waveguide to produce 100% reflected power. 1kW with the suitable gas flow rate produced appropriate temperatures while giving a reliable performance.

### **5.5.2 Gas Flow Rate**

The optimum plasma gas flow rate is determined by the power and the nozzle size. The following experiments used 1kW with a 0.5mm diameter nozzle aperture. Smaller apertures allow less gas to be used but the temperature at the tip of the nozzle is hotter and this increases the rate of erosion and can cause the tip to melt. The range for argon and nitrogen flow rates were found by experiment. Argon flow rates of 0.25 to 0.35 L/min resulted in a low velocity plasma jet. The temperature of the plasma jet is high because of the ratio of power to gas, but the buoyancy of the hot gas produces similar velocities, and results in a jet that bends upwards and does not reach the crucible. Lower flow rates cause instability because the jet can bend close enough to the plasma cavity that it jumps between the nozzle tip and the rim of the cavity opening and it can then enter the waveguide. Flow rates greater than 2L/min result in excess argon for the applied power. The high velocity means that there is less residence time in the electric field, so the resulting plasma jet is straight but too short to provide the required temperature at the crucible. 1.5L/min was chosen to give the required temperature and stability at 1kW. Table 5.1 show the summary of the gas flow rate and the temperature profiles. The nitrogen is

applied through the waveguide and is used to purge the gasifier and also to help to keep the hot gases and debris out of the plasma cavity. 2L/min was found to give reliable results. A 1kW plasma jet striking the crucible shown in Figure 5.6.

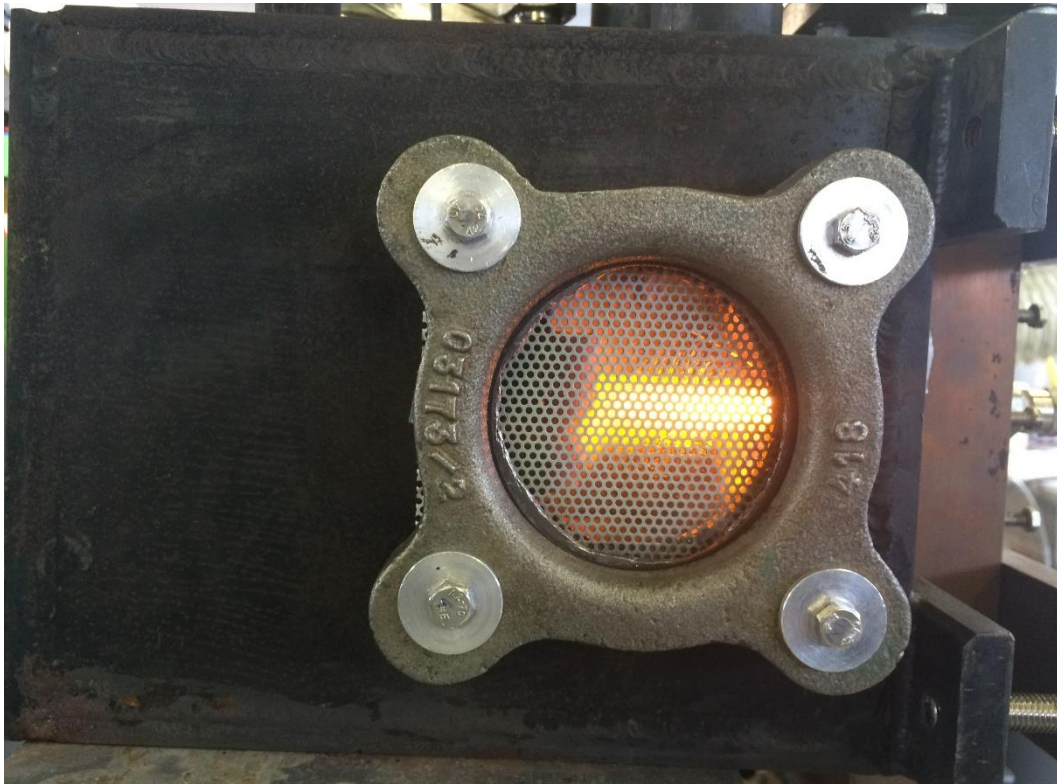


*Figure 5.6: 1kW Plasma in gasifier*

### **5.5.3 Pressure**

Pressure is required inside the gasifier to exclude air. It is produced by the temperature of the plasma but also by the gases produced by the sample. The pressure could be controlled within the range of the safety valve by manually adjusting the valve on the exhaust. The best results were obtained around 200mbar.

## 5.6 Plasma Temperature Profile

Table 5.1 shows the results for a set of experiment to monitor the temperature at the empty crucible. The argon was varied between 0.25L/min and 1.5L/min. The nitrogen was set with a ratio 1.4 relative to argon flow rate. The tests were performed with the gasifier at room temperature initially. 1kW applied for approximately 50min. The results are plotted in Figure 5.7.

Table 5.1: Argon, Nitrogen and Temperature Profile Test

	Argon (Ar) L/min	Nitrogen (N) L/min	Max Temperature °C
1	0.25	0.35	281.2
2	0.5	0.7	391.4
3	0.75	1.05	357.9
4	1	1.4	333.8
5	1.25	1.75	331.1
<b>6</b>	<b>1.5</b>	<b>2.1</b>	<b>420.2</b>

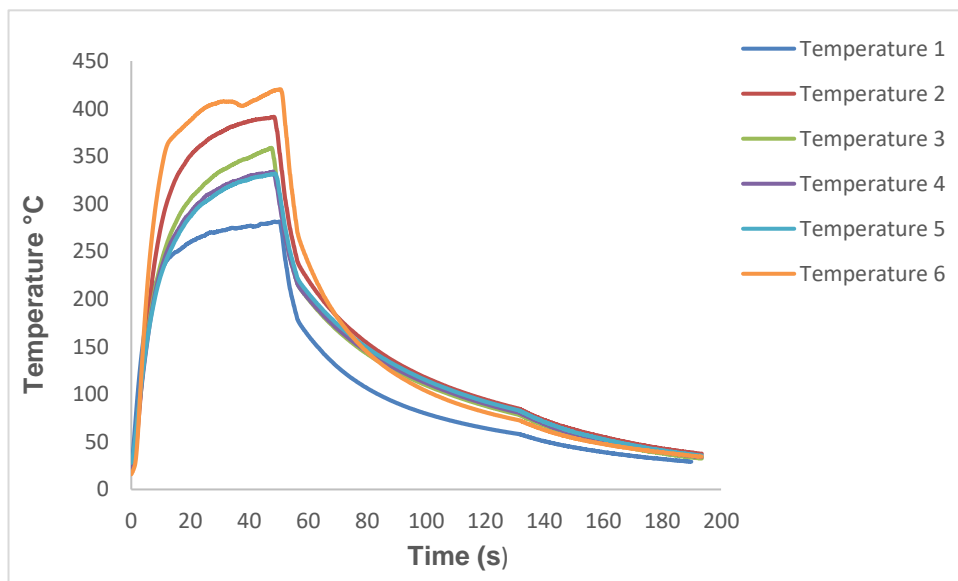
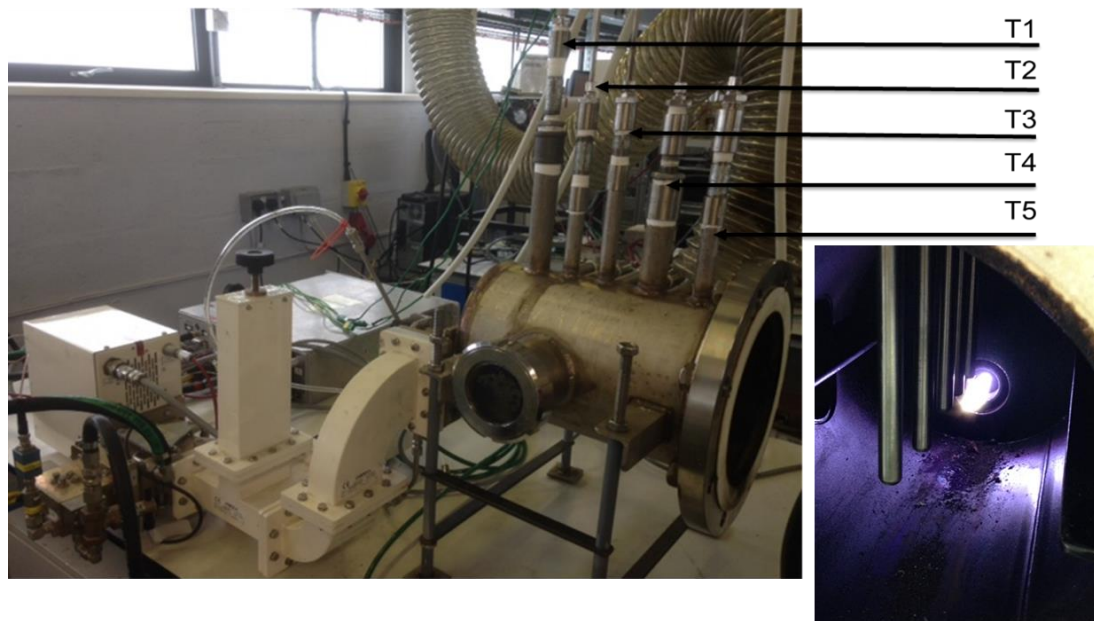


Figure 5.7: Plasma temperature profile at the box reactor

To give a better understanding of the plasma jet temperature a different reactor, shown in Figure 5.8, was also used. This cylindrical reactor had five thermocouples placed along the centre, at regular distances from the plasma cavity. The thermocouples were position 50mm above the nozzle height, so as not to impede the plasma jet.



*Figure 5.8: Temperature profile system*

PID control was developed in the LabView software so that the temperature at T3 was a constant 280°C. The results, Figure 5.9 show how the temperature of the other thermocouples vary, based on their location compared to T3, and also as the argon flow rate decreased, which was done once the temperature were settled ( $\pm 1^\circ\text{C}$ ). This took between 30 and 60 min.

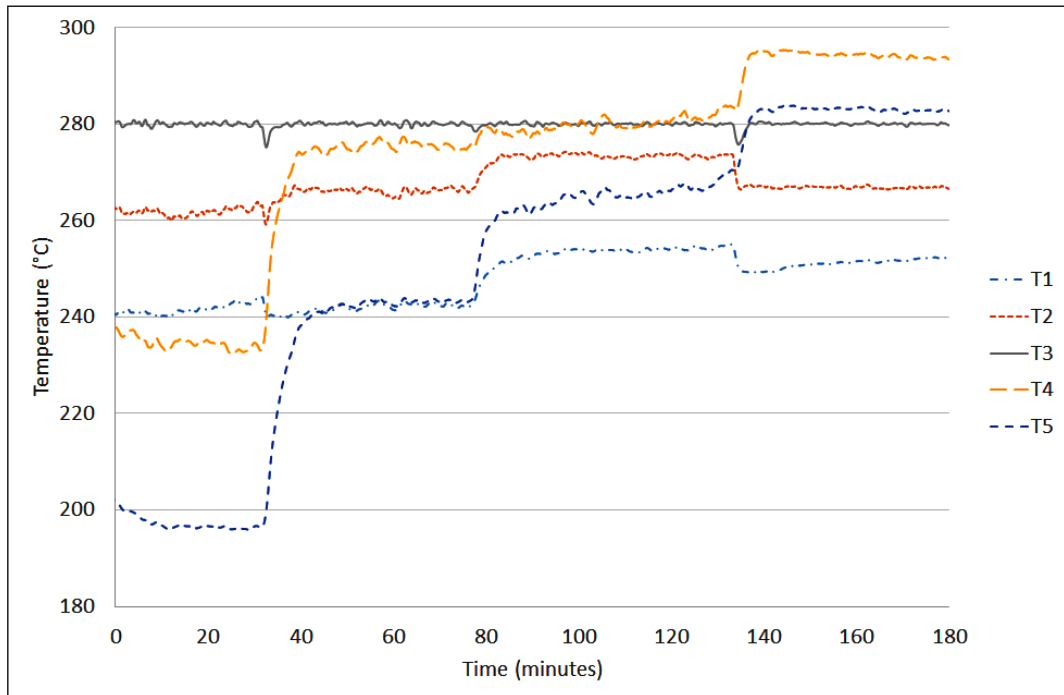


*Figure 5.9: Temperatures recorded by the thermocouples under different power and flow rates*

T1 and T5 generally gave the lowest temperatures. T1 was closest to the plasma cavity but the vertical offset meant that the plasma tended to pass below it. T5 was the furthest away but began to register high temperatures as the length of the plasma increased at the lower argon flow rates. All the thermocouples measured their highest temperatures when the upward bend of the plasma jet coincided with the thermocouple position.

## 5.7 Gas analysis

The gas needed to be filtered before the analyser could measure it. The gas Drierite purifier, shown in Figure 5.10, was used to filter the dirty gas before it went to the Quintox unit. This gas purifier is designed for gas chromatography and it will filter gases used for chromatography and spectrometry. The purifier

is filled with washed soft sand, and removed moisture and particulates from the gas line.

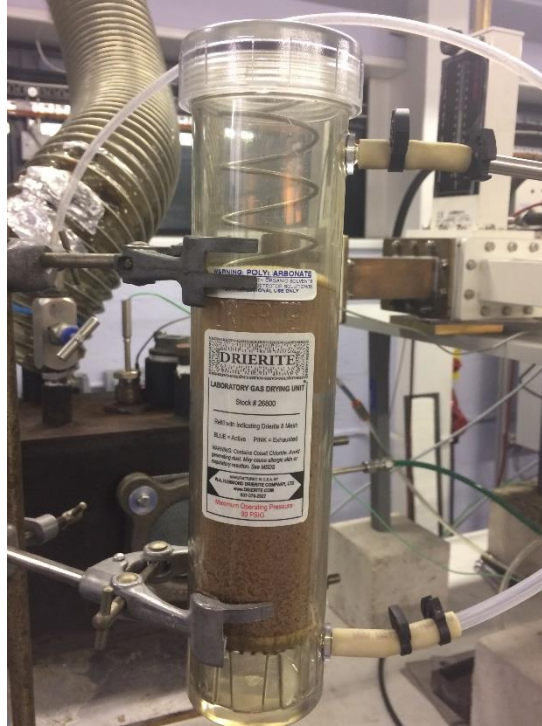


*Figure 5.10: Drierite Unit*

The output gases were sampled using a 8mm clear flexible tube connected to a T-piece on the top of the reactor exhaust. This tube made it easy to monitor any condensation or tar build up. The Labview software captured the gas data every 10s.

## 5.8 Chapter Summary

This chapter explained details of the sample preparation for the pyrolysis/gasification tests. The waste samples were ground to a uniform consistency using a blender. The key parameters of the feedstock: moisture content, ash content, volatile matter content, elemental composition and calorific value were investigated.

The experimental operating conditions and parameters such as power level, argon and nitrogen flow rates and pressure are discussed. The temperature and gas flow profiles are provided. Chapter Six will explain about the results, analysis and discussion.

## RESULTS, ANALYSIS AND DISCUSSION

### 6 : Introduction

Waste samples were collected from a Byron Hamburger restaurant in Liverpool. The waste was sorted into food waste and paper waste. 3kg of waste from each category was sent to an external laboratory for analysis (Knight Energy Services Limited). The results are shown in Table 6.1 and Table 6.2.

*Table 6.1: Food Waste Analysis*

	As Received	Dry Basis	Dry Ash-Free	
Total Moisture	52.3			%
Ash Content	2.0	4.1		%
Volatile Matter	40.4	84.6	88.2	%
Fixed Carbon	5.4	11.3	11.8	%
Total Sulphur	0.09	0.19	0.2	%
Chlorine	0.72	1.51	1.57	%
Carbon	28.9	60.6	63.2	%
Hydrogen	4.06	8.51	8.87	%
Nitrogen	1.50	3.14	3.27	%
Oxygen by difference	10.5	22	22.9	%
Gross Calorific Value	12.06	25.283	26.364	MJ/kg
Net Calorific Value	9.912			MJ/kg

Table 6.2: Paper Waste Analysis

	As Received	Dry Basis	Dry Ash-Free	
Total Moisture	18.8			%
Ash Content	1.3	1.6		%
Volatile Matter	70.7	87.1	88.5	%
Fixed Carbon	9.2	11.3	11.5	%
Total Sulphur	0.11	0.13	0.13	%
Chlorine	0.2	0.25	0.25	%
Carbon	37.7	46.4	47.2	%
Hydrogen	5.19	6.39	6.49	%
Nitrogen	0.27	0.33	0.34	%
Oxygen by difference	36.5	44.9	45.6	%
Gross Calorific Value	14.669	18.065	18.359	MJ/kg
Net Calorific Value	13.08			MJ/kg

The modified Dulong equation (6.1) [89] can be used to approximate the gross calorific value based on carbon, hydrogen, oxygen and sulphur measurements.

$$Q = 4.18 \left( 78.4C + 241.3 \left( H - \frac{O}{8} \right) + 22.1S \right) \quad (6.1)$$

where

- C = Mass % of carbon
- H = Mass % of hydrogen
- O = Mass % of oxygen
- S = Mass % of sulphur

This equations gave values of 12.25 MJ/kg and 13.00 MJ/kg. The error is larger for the paper waste because the oxygen is higher than the 10% limit which usually applies for the coefficients used.

## 6.1 Sample Moisture Properties

To find the moisture content in the laboratory, three samples of mixed food, paper waste and fries waste were placed in crucibles in the laboratory oven at 105°C. The sample mass was 10g for mix waste and fries waste but for the paper waste 4g was used because 10g would not fit in the aluminium crucible.

*Table 6.3: Data obtained during drying process*

Sample	Empty (g)	Full Wet (g)	Full Dry(g)				
			(1)	(2)	(3)	(4)	(5)
<b>MF1</b>	3.645	13.645	11.236	9.964	9.685	9.578	9.529
<b>MF2</b>	3.638	13.638	11.138	9.721	9.454	9.359	9.318
<b>MF3</b>	3.697	13.697	11.109	9.552	9.1	8.865	8.773
<b>PN1</b>	3.687	7.857	7.599	7.549	7.533	7.525	7.519
<b>PN2</b>	3.641	7.466	7.438	7.391	7.371	7.368	7.362
<b>PN3</b>	3.642	7.792	7.548	7.501	7.481	7.48	7.473
<b>FR1</b>	3.656	13.656	11.17	10.256	10.153	10.106	10.081
<b>FR2</b>	3.568	13.568	11.156	9.766	9.6	9.54	9.509
<b>FR3</b>	3.664	13.664	11.176	9.93	9.796	9.747	9.72

(MF=Mix Food) (PN=Paper Napkin) (FR=Fries)

Before starting the measurement, the empty crucible mass was recorded and then the 10g sample was added into it. Once weighed, the nine samples were placed inside the laboratory oven. The measurement was recorded until the difference in mass for all the samples was below 0.1g, as shown in Table 6.3.

*Table 6.4: Moisture content calculation*

<b>Feedstock</b>	<b>Original Mass (g)</b>	<b>Dried Mass (g)</b>	<b>Moisture Content (%)</b>
<b>MF 1</b>	13.645	9.529	43.19
<b>MF2</b>	13.638	9.318	46.36
<b>MF3</b>	13.697	8.773	56.13
		<b>mean</b>	<b>48.56</b>
<b>PN1</b>	7.857	7.519	4.49
<b>PN2</b>	7.466	7.362	1.41
<b>PN3</b>	7.792	7.473	4.26
		<b>mean</b>	<b>3.39</b>
<b>FR1</b>	13.656	9.6	42.25
<b>FR2</b>	13.568	9.509	42.68
<b>FR3</b>	13.664	9.72	40.57
		<b>mean</b>	<b>41.83</b>

(**MF**=Mix Food) (**PN**=Paper Napkin) (**FR**=Fries)

Table 6.4 shows the Moisture content calculation for all the wastes sample. The moisture content calculated for mixed food waste was 48.56% which similar to the Knight Energy analysis of 52.3%. The paper waste in the laboratory was only 3.39%, which was much lower than the Knight Energy

value of 18.8%, but this will depend on whether the napkins have absorbed water from food waste. The fries had a mean moisture content of 41.83%, which is less than the mix food values.

## 6.2 System Experimentation

Gasification experiments were carried out on these mixed food, fries and paper waste samples. as shown in Figure 6.1. Table 6.5 shows the mass of ash after the samples were gasified, and the percentage ash compared to the original wet and dry masses.

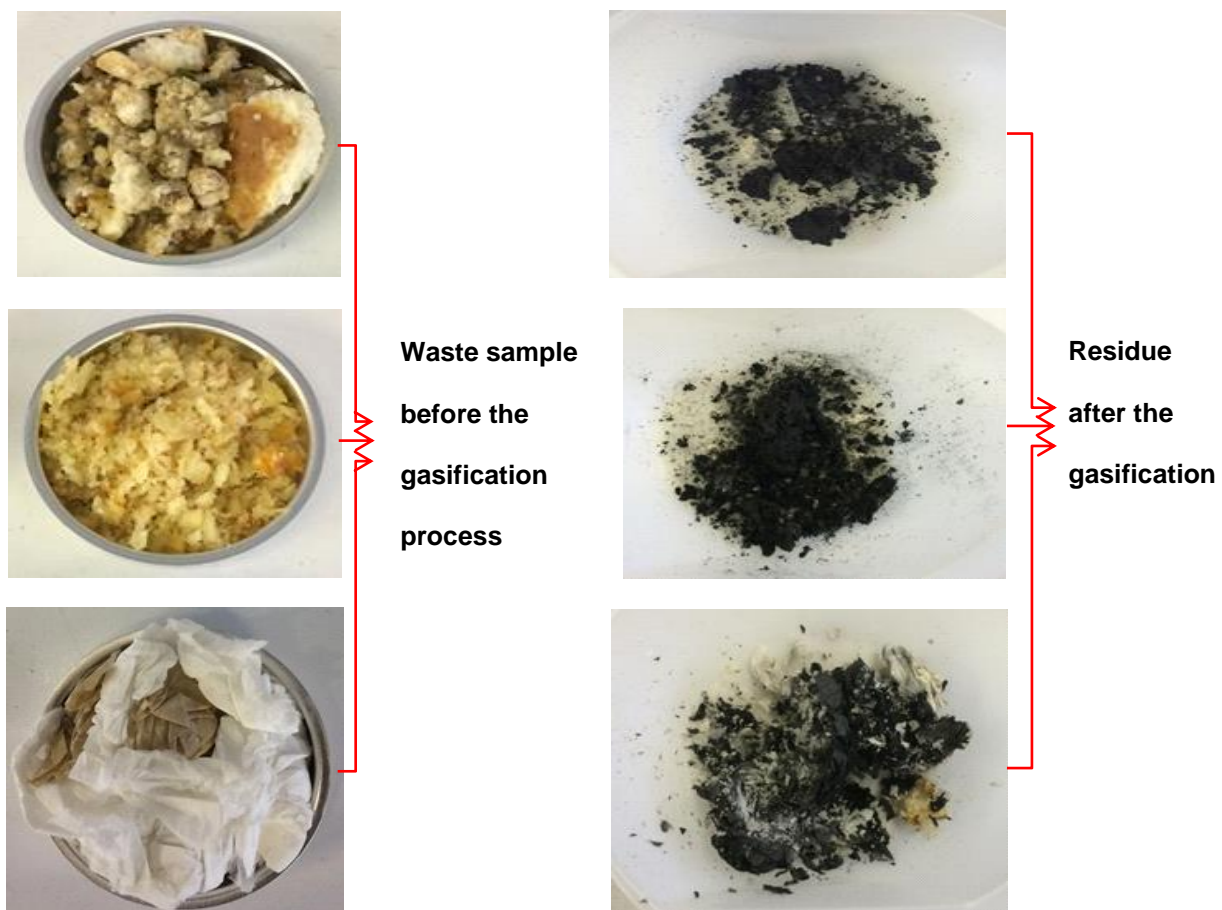


Figure 6.1: Samples before and after the gasification process.

Table 6.5: Ash content calculation

Sample	Ash		
	mass (g)	(wet basis) (%)	(dry basis) (%)
<b>MF 1</b>	0.33	2.4	5.6
<b>MF2</b>	0.73	5.4	12.9
<b>MF3</b>	0.74	5.4	14.6
<b>PN1</b>	0.67	8.5	18.3
<b>PN2</b>	0.5	6.7	12.8
<b>PN3</b>	0.6	7.7	16.3
<b>FR1</b>	0.54	4.0	9.1
<b>FR2</b>	0.68	5.0	11.4
<b>FR3</b>	0.61	4.5	10.1

(**MF**=Mix Food) (**PN**=Paper Napkin) (**FR**=Fries)

These values are much larger than the Knight Energy analysis results. It is clear from Figure 6.1, that there is a large amount of carbon left after the test.

The weight (%) from three different gasified ash content samples, as shown on Table 6.5, were calculated to be compared with the quantified results obtained from the scanning electron microscopy equipped with energy dispersive X-ray analysis (SEM-EDX) in order to identify and quantify the elemental constituents in three waste categories. Nine different essential chemical elements for each sample were found in the mixed food, paper/napkin and fries samples (Figure 6.2, 6.3 and 6.4),

### 6.2.1 EDX for Results for Mix Food Waste

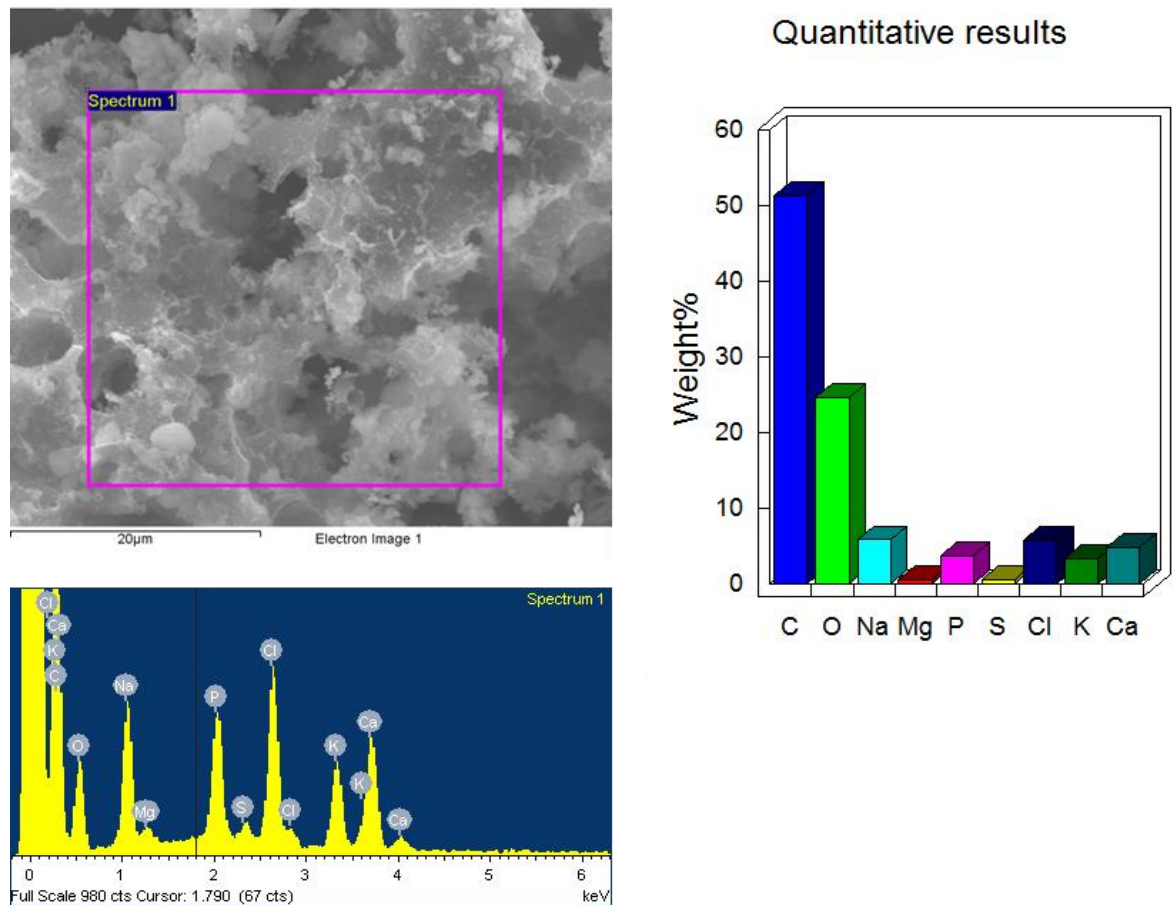


Figure 6.2: EDX results for mixed food ash.

Figure 6.2 shows that there was 51.25% carbon and 0.52% sulphur by weight, left in the mixed food ash sample. The others elements detected were sodium (5.76%), magnesium (0.47%), phosphorus (3.73%), chlorine (5.75%), potassium (3.24%) and calcium (4.72%).

The carbon gave a high percentage because the gasification temperature did not reach 600°C and may have lacked the necessary free oxygen. Some of the oxygen detected in the ash will exist as oxides of calcium (CaO), sodium (Na<sub>2</sub>O), potassium (K<sub>2</sub>O) and magnesium (MgO). The atomic percentages for these metals is found by dividing the weight% by the atomic weight and

dividing by the sum of these results for all the elements present. The atomic% for calcium, sodium, potassium and magnesium are 1.79, 3.81, 1.83 and 0.29 respectively. This would however only account for a maximum atomic% of  $1.79 + 0.5(3.81 + 1.83) + 0.29 = 4.9$  for oxygen. It is probable that most of the oxygen actually occurs as phosphates, sulphates and carbonates. Calcium carbonate ( $\text{CaCO}_3$ ), for example, would account for 5.37% of the oxygen if it did not decomposed to calcium oxide. The measured atomic% of oxygen is 23.36 as the weight% is 24.56%.

### 6.2.2 EDX Result for Paper/Napkin Waste

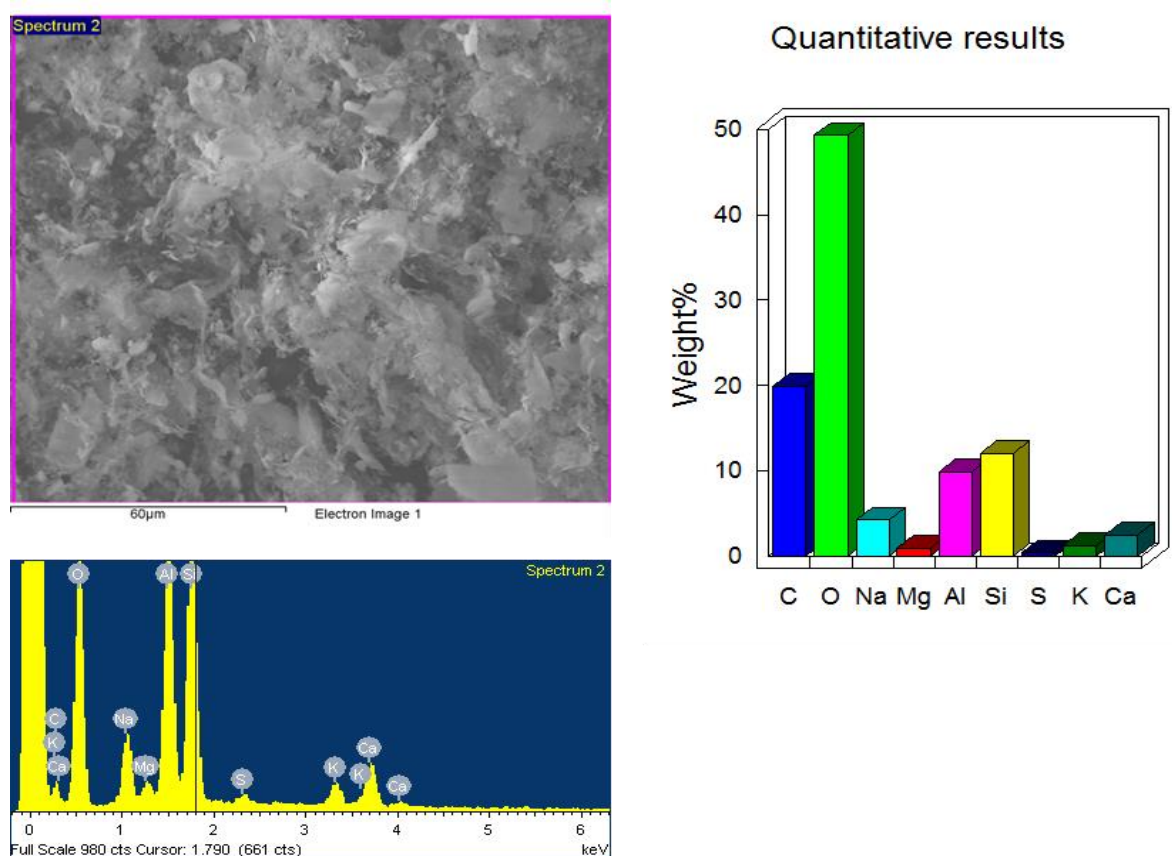


Figure 6.3: EDX results for Paper/Napkin ash.

Figure 6.3 shows the carbon and sulphur were lower for the napkin and paper waste at 19.87% and 0.36% sulphur respectively. The others elements detected were sodium (4.18%), magnesium (0.87%), aluminium (9.82%), (12%) silicon, (1.18%) potassium and calcium (2.4%). Chlorine only appears in the mixed food results. This indicates that it mostly occurs because of the salt (NaCl) in the food. The chemical composition of the paper waste (Table 6.2) did show some chlorine but it was 3.6 times lower than in the mixed food, and this may have been partly been due to contact with food waste.

Possible oxides would include CaO, Na<sub>2</sub>O, K<sub>2</sub>O, MgO, SiO<sub>2</sub>, Al<sub>2</sub>O<sub>3</sub>. The maximum atomic% for oxygen based on these compounds would be

$$1.02+0.5(3.11+0.51)+0.61+2(7.31)+1.5(6.23) = 27.4\%.$$

The measured atomic % of oxygen is 52.72%, so metal phosphates, sulphates and carbonates are likely to have remained.

### 6.2.3 EDX Result for Fries/Chips Waste

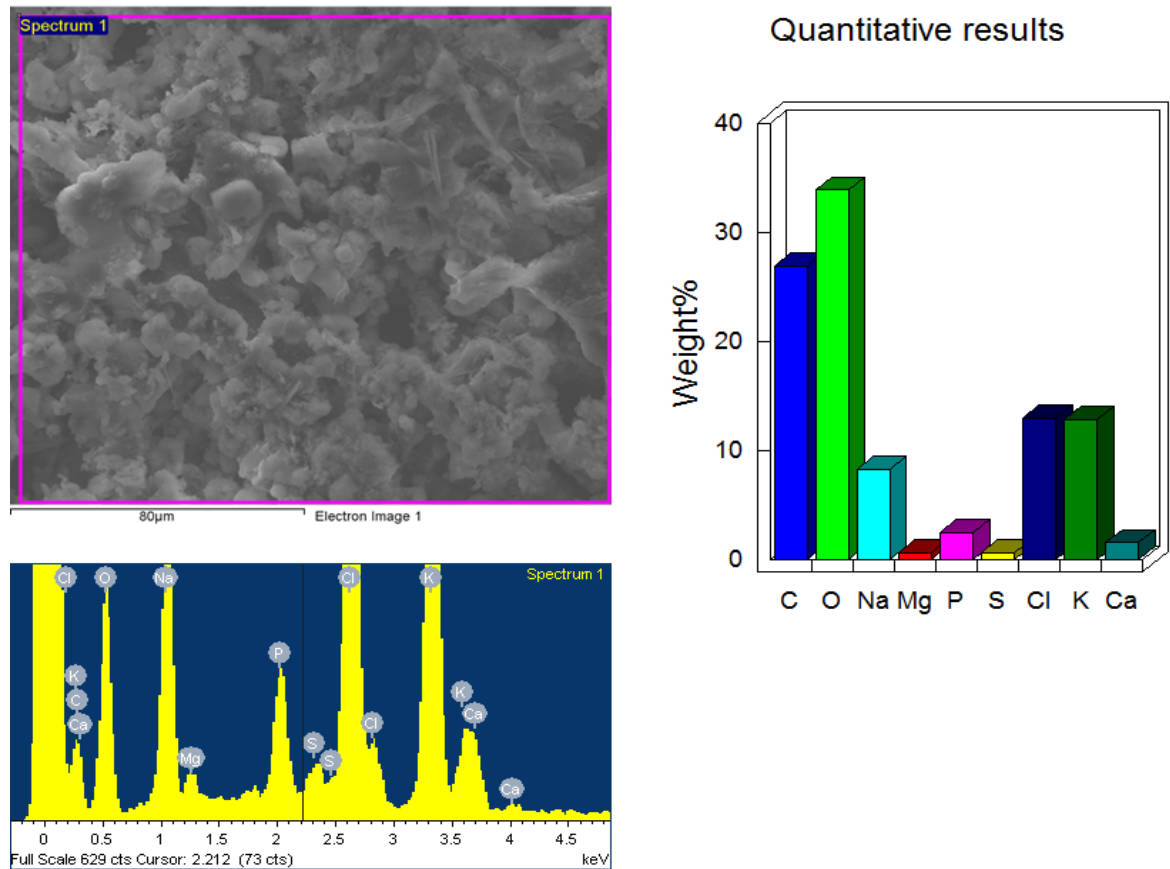


Figure 6.4: EDX results for Fries/chip ash

Figure 6.4 shows the carbon and sulphur for the fries waste was 26.91% and 0.59% sulphur respectively. The others elements detected were sodium (0.59%), magnesium (0.61%), phosphorus (2.42%), chlorine (12.97%), potassium (12.83) and calcium (1.54%).

Possible oxides would include CaO, Na<sub>2</sub>O, K<sub>2</sub>O and MgO, so the maximum atomic % for oxygen would be  $0.69 + 0.5(6.42 + 5.89) + 0.45 = 7.3\%$ .

The measured atomic % of oxygen is 38.04%. Sodium sulphate (Na<sub>2</sub>SO<sub>4</sub>) could account for 12.84% of the oxygen and there may not have been sufficient temperature to decompose to the sulphide as shown in equation (6.2).



### 6.3 Plasma Treatment of Waste

Triplicate 60 minute tests were carried out for each of the waste samples in the microwave plasma reactor. Figure 6.5 and Figure 6.6 show the masses for the empty crucible, and after the 10g sample was added.



Figure 6.5: Empty crucible weight



Figure 6.6: Crucible + sample weight

Figure 6.8 shows the vapour condensing on the sight glass. Figure 6.9 shows smoke formation in the gasifier, Figure 6.10 shows the plasma jet as the smoke dissipates, while Figure 6.11 and Figure 6.12 show the colour change in the plasma jet as syngas production in the gasifier reduces.



Figure 6.7: Dark yellow plasma



Figure 6.8: Vapour formation



Figure 6.9: Smoke formation

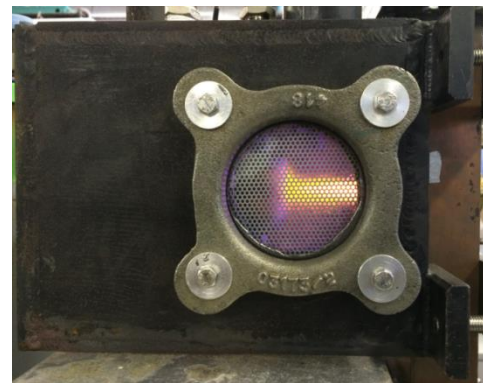


Figure 6.10: Flame reduced, more smoke



Figure 6.11: Reduced smoke



Figure 6.12: No visible smoke

Table 6.6 shows the forward and reflected powers at 10 min intervals together with the observations of the plasma jet.

*Table 6.6: Observation monitoring during the experiment*

TIME	FP	RF	ARGON	NITROGEN	COMMENTS
0	1.00± 0.02	0.01	1.5	5	Start/Yellow
10	1.00± 0.02	0.01	1.5	5	Yellow/Smoke/Steam
20	1.00± 0.02	0.01	1.5	5	Yellow/Steam↓
30	1.00± 0.02	0.01	1.5	5	Bright Yellow
40	1.00± 0.02	0.03	1.5	5	Yellow/Spike
50	1.00± 0.02	0.03	1.5	5	Yellow
60	1.00± 0.02	0.02	1.5	5	End

### 6.3.1 Gas Analysis

This experimental work was carried out with a self-striking plasma as described in section 5.6. All the tests began at room temperature, which was in the range  $22^{\circ}\text{C} \pm 2^{\circ}\text{C}$ . The samples were placed in the crucible and the sight glass was sealed. The microwave power was switched on and set to 1kW, and the tuner was adjusted to the position at which the plasma struck. The tuner was then readjusted to achieve minimum reflective power. Each experiment was carried out for 60 minutes. After this period the power was switched off, and the reactor was left to cool. The sight glass remained in place until the reactor was at room

temperature. The external temperature was measured to indicate the losses from the box reactor.

While these reactions were underway, the production of CO<sub>2</sub> and CO was detected, in addition to O<sub>2</sub>, by the gas analyser. The CO<sub>2</sub> and CO were kept in balance by the water gas shift (WGS) reaction. The reaction is slightly exothermic, and is not significantly disrupted below temperatures of approximately 240°C.

### 6.3.2 Mixed Food Results

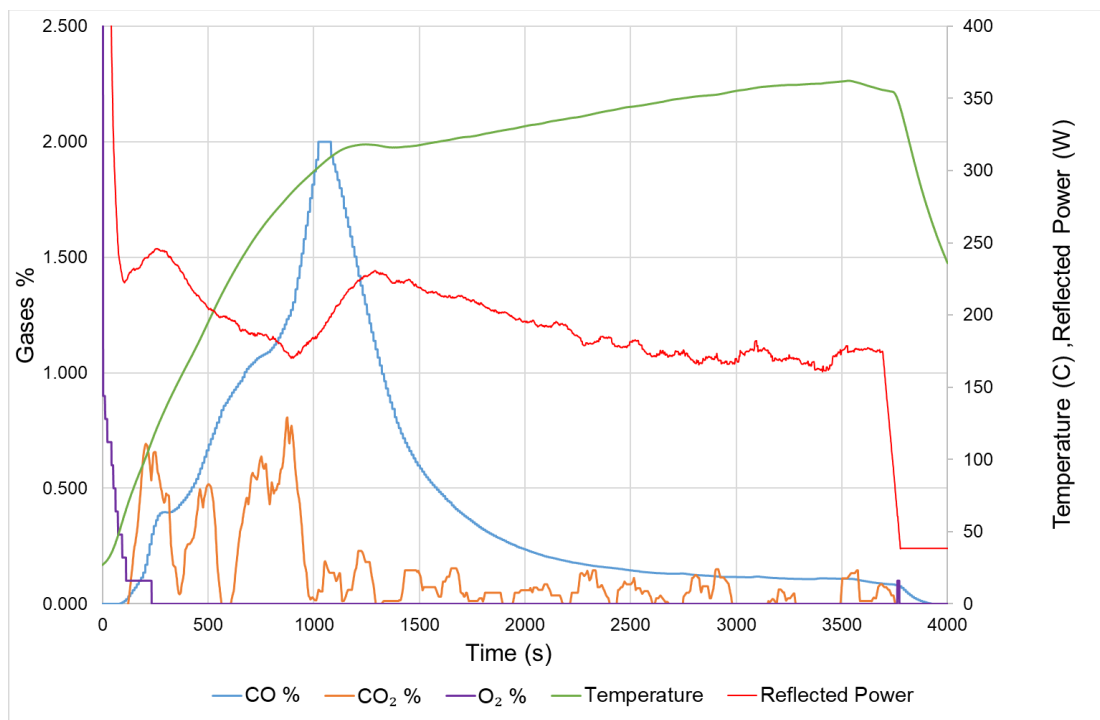


Figure 6.13: Results for Mixed Food (1)

Three repetitions for 10g samples of mixed food waste material were carried out. Figure 6.13 shows the first of these results. The blue line indicates CO%, the purple line indicates the O<sub>2</sub>%, the orange line indicates CO<sub>2</sub>%. The green line indicates the inside temperature profile and the red line indicates the

reflected power. Due to the presence of a small % of  $O_2$ , the  $CO_2$  is initially higher than  $CO$ . After approximately 800s, the  $CO$  value begins to increase rapidly, while the  $CO_2$  drops to lower value of around 0.1%. The  $CO\%$  plateaus at 2%, despite the increased flow of nitrogen, as this is the upper limit of the gas analyser limit. At this point the ratio of  $CO$  to  $CO_2$  is at least 20:1. The mixed waste food contains high calories and is comparatively wet. This caused the plasma to be disturbed during the experiment, which also caused the temperature to briefly drop at approximately 10 minutes in. The temperature inside the reactor reached  $362^\circ C$  by the end of this test.

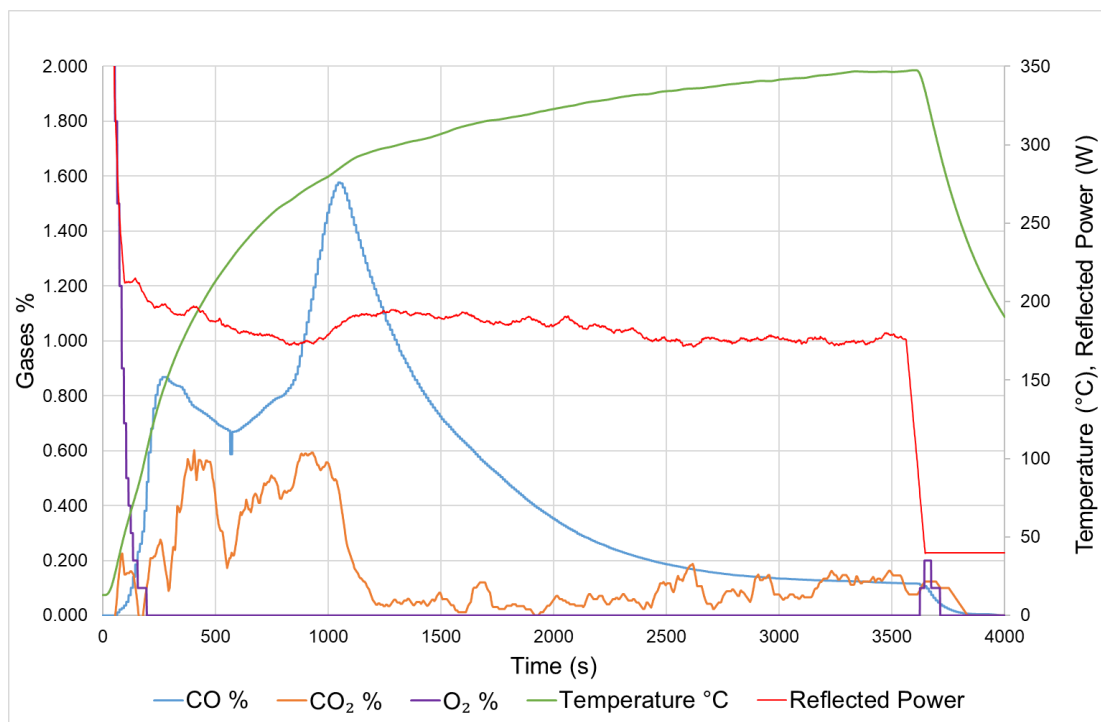
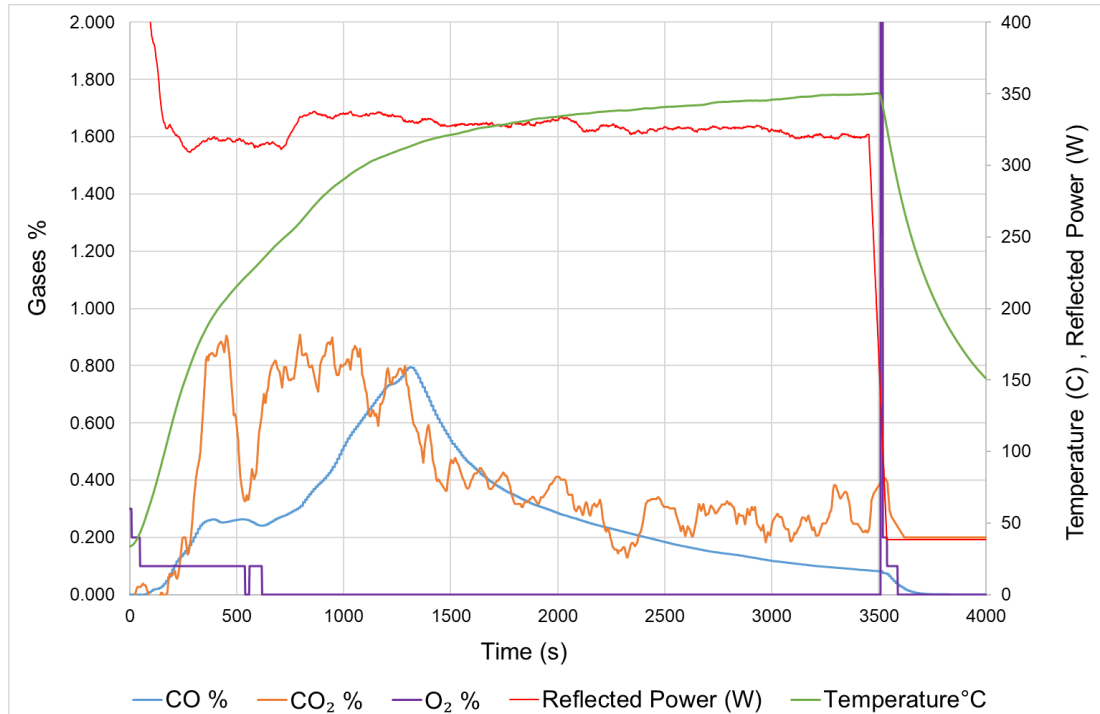


Figure 6.14: Results for Mixed Food (2)

Figure 6.14 shows the second experiment of the mixed food results. Similar features to the previous experiment are seen, however the  $CO\%$  measurement only reach 1.58%. The initial  $O_2$  was higher in this test, and this cause more

CO<sub>2</sub> to be produced. This will have also reduced the CO% as available carbon is reduced. The temperature reached a maximum of 347°C for this test.



*Figure 6.15: Results for Mixed Food (3)*

Figure 6.15 shows the gas analysis, temperature and reflected power for the mixed food waste (3). The O<sub>2</sub>% remained at 0.1% until about 500s into the test. Compared from the previous graph, the peak CO% measurement was lower than the previous tests, and only reach 0.8%. This was due to the additional oxygen and the increased production of CO<sub>2</sub>% that occurred. CO<sub>2</sub>% reached a maximum 0.9%. The reflected power level was slightly high in this test, this was required to get the plasma to strike and remain stable throughout the experiment.

### 6.3.3 Fries

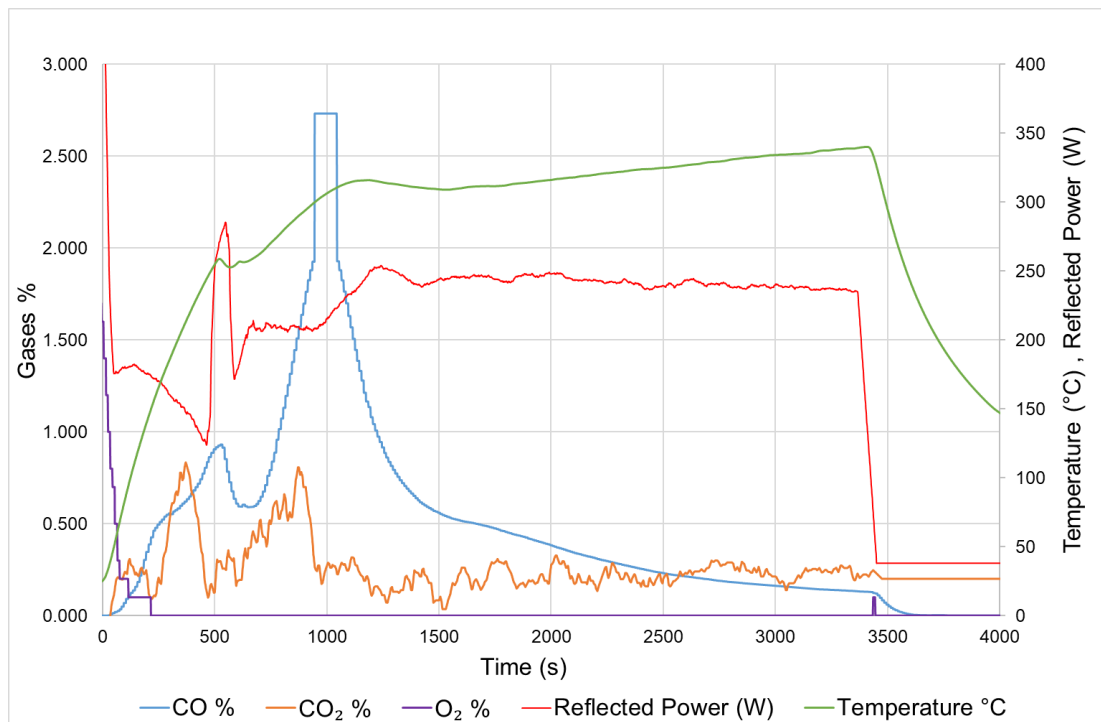
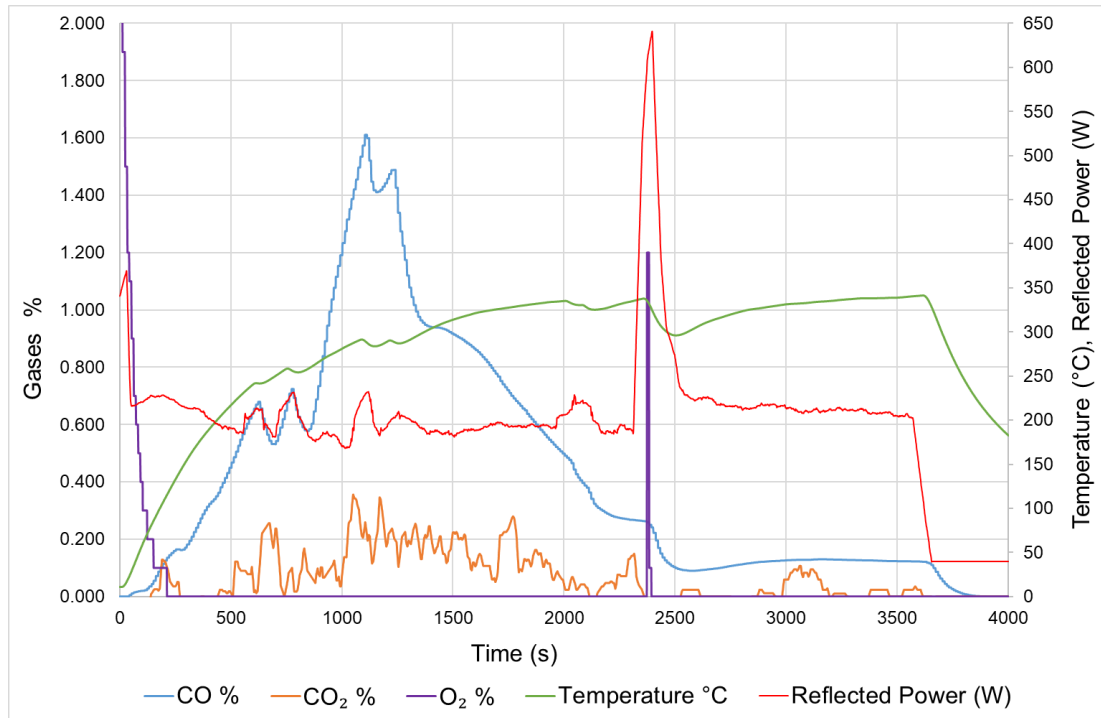


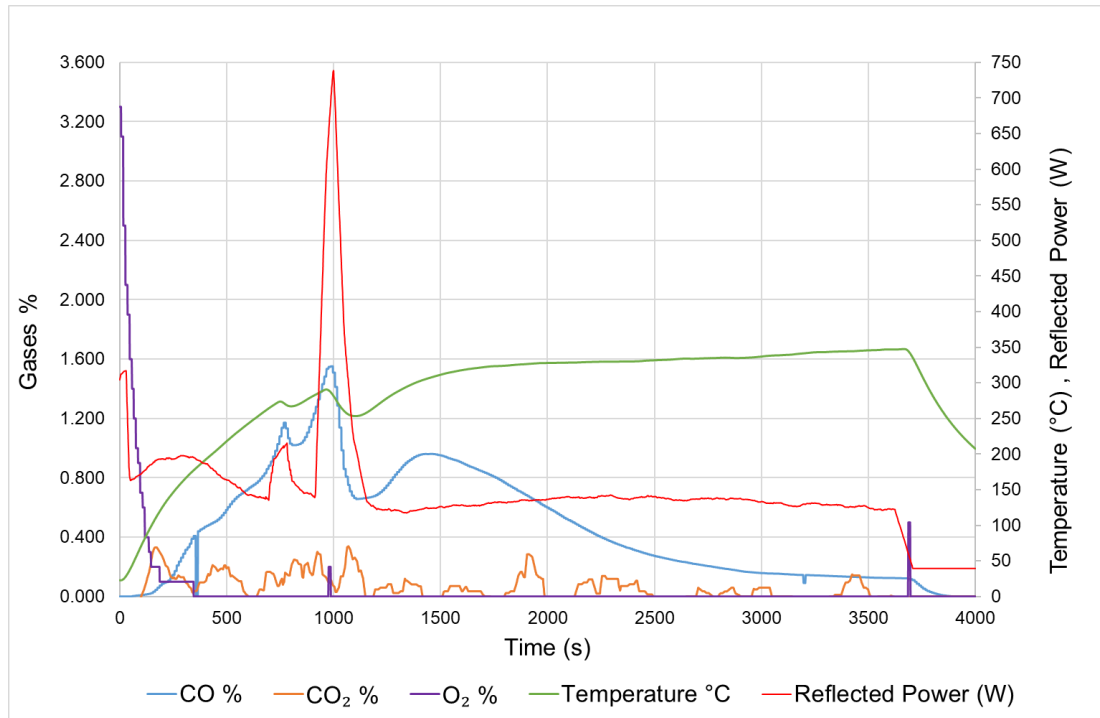
Figure 6.16: Results for Fries/Chip (1)

Figure 6.16 shows the first result for the fries/chip waste sample. The level of O<sub>2</sub>% is still dropping when the experiment begins. The CO% also reached the 2% limit of the gas analyser. The oil in the fries/chip produces a lot of smoke, and all three tests suffered with plasma instabilities as indicated by sudden changes in the reflected power measurements and corresponding reductions in temperature. CO<sub>2</sub>% generate up to 0.7% from this waste sample



*Figure 6.17: Results for Fries/Chip (2)*

Figure 6.17 shows the second result of the fries/chip experiment. This time the CO% developed over a longer time and the maximum value of 1.6% was smaller as a result. The plasma was particularly unstable during this test. There was plasma instability at approximately 2350s. This is evidenced by the jump in reflected power. The corresponding jump in O<sub>2</sub>% is believed to be due to electrical activity rather than a true increase. The plasma was re-struck but the system did not perform very stable. This causes the temperature drop inside the reactor and the experiment was continued for the remaining time to complete the full cycles.



*Figure 6.18: Results for Fries/Chip (3)*

Figure 6.18 shows the gas analysis, temperature and reflected power for the fries/chip (3). There were instabilities with the plasma between 500s and 1000s, which will have been caused by the production of smoke. The plasma was re-struck, and this again produced a brief increase in O<sub>2</sub>, which supports the conclusion from the previous test.

### 6.3.4 Paper/Napkin

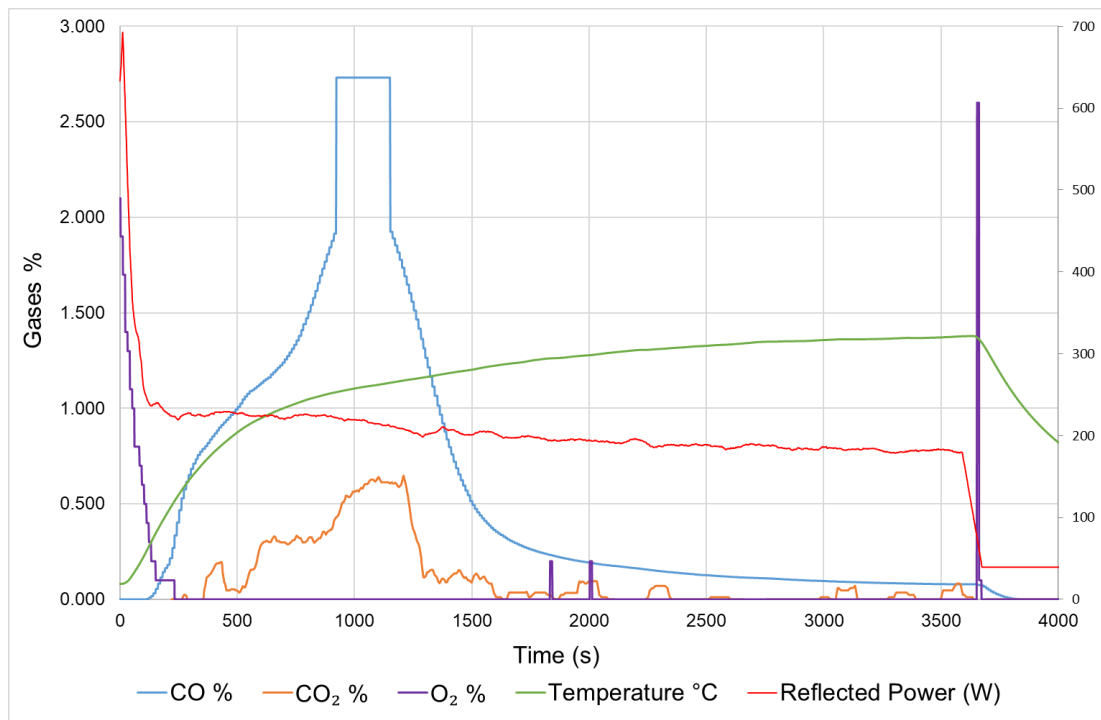
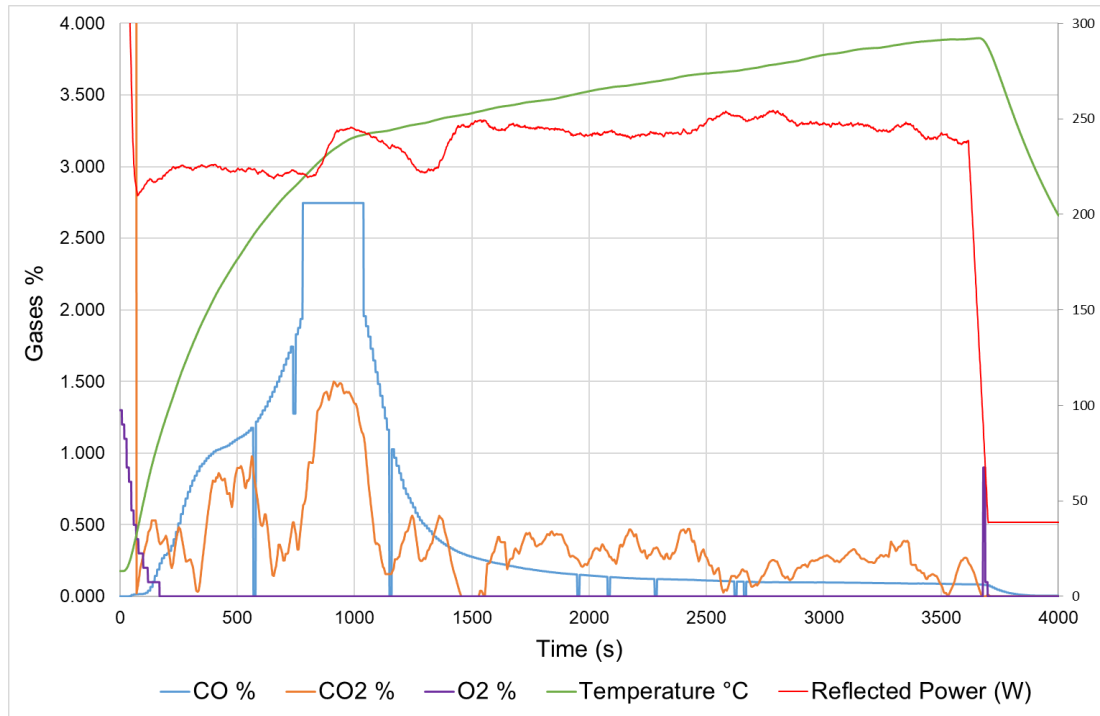


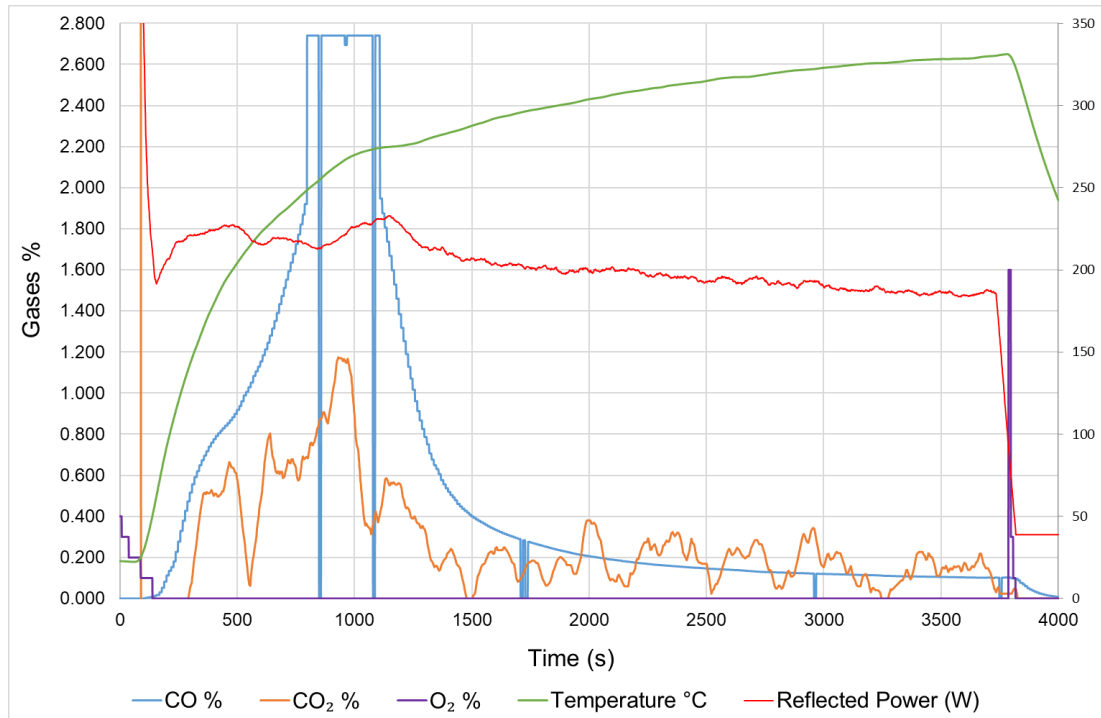
Figure 6.19: Results for Paper/Napkin (1)

Figure 6.19 shows the first result for the paper/napkin waste sample. Three repetition of experiment were also carried out using samples of this waste material. Compared with the previous waste feedstock, this waste material was relatively dry and the plasma was very stable during the experiment as shown by the reflected power.



*Figure 6.20: Results for Paper/Napkin (2)*

Figure 6.20 shows the second result of the paper/napkin experiment. The reflected power measurement slightly high on this experiment compare with the first experiment. The CO<sub>2</sub> % was measured up to 1.5 % higher compare with experiment (1) and (2).



*Figure 6.21: Results for Paper/Napkin (3)*

Figure 6.21 shows the gas analysis, temperature and reflected power for the paper/napkin (3). The CO<sub>2</sub> % was measured slightly lower compare with experiment (2).

Table 6.7 shows the total of gas measurement during the experiments. As the production of gases for each repetition are different, it is not possible to simply compare peak values. Instead, the actual amount of gas produced, has been calculate by integrating the gas data by summing the results over the one hour period. The total volumes of gas produced in 3600s are indicates in bold number while the volumes of gas produce, including the cooling period are shown in brackets.

*Table 6.7: Summary of the Total Gas Measurements*

	<b>CO</b> (3600s/End of Test)	<b>CO<sub>2</sub></b> (3600s/End of Test)	<b>O<sub>2</sub></b> (3600s/End of Test)
<b>MF(1)</b>	<b>1221.4</b> (1230.0)	<b>319.8</b> (303.1)	<b>13.4</b> (14.1)
<b>MF(2)</b>	<b>1248.5</b> (1253.4)	<b>409.8</b> (420.7)	<b>56.3</b> (61.5)
<b>MF(3)</b>	<b>695.9</b> (696.3)	<b>1032.4</b> (1413.4)	<b>79.9</b> (79.9)
<b>FR(1)</b>	<b>1338.8</b> (1339.1)	<b>638.4</b> (703.4)	<b>58.5</b> (58.5)
<b>FR(2)</b>	<b>1163.5</b> (1172.3)	<b>167.5</b> (167.5)	<b>85.9</b> (85.9)
<b>FR(3)</b>	<b>1268.6</b> (1281.5)	<b>161.3</b> (160.6)	<b>128.2</b> (131.7)
<b>PN(1)</b>	<b>1505.8</b> (1508.1)	<b>269.4</b> (269.4)	<b>43.9</b> (43.9)
<b>PN(2)</b>	<b>1362.9</b> (1372.0)	<b>959.1</b> (959.1)	<b>26.5</b> (60.8)
<b>PN(3)</b>	<b>1465.5</b> (1479.2)	<b>68.5</b> (686.4)	<b>2.2</b> (16.2)

These results are useful for showing how, despite the different shapes of the graph, that the total amount of CO produced for each waste stream is similar. The only significant exception being for mixed food 3.

### **6.3.5 Mass Measurements Mixed Food**

#### **6.3.5.1 Result of Experiment 1**

Empty Crucible=**333.21g**

Start weight = **343.21g**

End weight = 333.54-333.21 (crucible) = **0.33 g**

Mass of residue= 0.33/10 x 100=**3.3% w/w**

Percentage reduction in mass= (100-3.3) = **96.7%**

### **6.3.5.2 Result of Experiment 2**

Empty Crucible=**333.20g**

Start weight = **343.20**

End weight = 333.93-333.20 (crucible) = **0.73 g**

Mass of residue= 0.73/10 x 100=**7.3% w/w**

Percentage reduction in mass= (100-7.3) = **92.7%**

### **6.3.5.3 Result of Experiment 3**

Empty Crucible=**333.20g**

Start weight = **343.20**

End weight = 333.94-333.20 (crucible) = **0.74 g**

Mass of residue= 0.74/10 x 100=**7.4% w/w**

Percentage reduction in mass= (100-7.3) = **92.6%**

*Table 6.8: Mass change of each mix food sample in response to microwave pyrolysis treatment*

<b>Experiment</b>	<b>1</b>	<b>2</b>	<b>3</b>
<b>Start mass (g)</b>	10.00g	10.00g	10.00g
<b>End mass (g)</b>	0.34	0.73	0.74
<b>Total loss (g)</b>	9.66	9.27	9.26

Table 6.8 shows the start and final mass of the mixed food waste. The samples were not pre-dried. 10g mass were used for the experiment and a mean reduction of 94.0% was observed, with a standard deviation of 2%.

### 6.3.6 Mass Measurements Fries/Chips

#### 6.3.6.1 Result of Experiment 1

Empty Crucible=**333.20g**

Start weight = **343.20g**

End weight = 333.74-333.20 (crucible) = **0.54 g**

Mass of residue=  $0.33/10 \times 100$ =**5.4% w/w**

Percentage reduction in mass=  $(100-5.4)$  =**94.6%**

#### 6.3.6.2 Result of Experiment 2

Empty Crucible=**333.20g**

Start weight = **343.20**

End weight = 333.88-333.20 (crucible) = **0.68 g**

Mass of residue=  $0.68/10 \times 100$ =**6.8% w/w**

Percentage reduction in mass=  $(100-7.3)$  =**93.2%**

#### 6.3.6.3 Result of Experiment 3

Empty Crucible=**333.20g**

Start weight = **343.20**

End weight = 333.81-333.20 (crucible) = **0.61 g**

Mass of residue=  $0.61/10 \times 100$ =**6.1% w/w**

Percentage reduction in mass=  $(100-6.1)$  =**93.9%**

*Table 6.9: Mass change of each fries/chips sample in response to microwave pyrolysis treatment*

<b>Experiment</b>	<b>1</b>	<b>2</b>	<b>3</b>
<b>Start mass (g)</b>	10.00g	10.00g	10.00g
<b>End mass (g)</b>	0.54	0.68	0.61
<b>Total loss (g)</b>	9.46	9.32	9.39

Table 6.9 shows the start and final mass of the fries/chips waste. The samples were not pre-dried. 10g mass were used for the experiment and a mean reduction of 93.9% was observed, with a standard deviation of 1%.

### **6.3.7 Mass Measurements Paper/Napkin Waste.**

#### **6.3.7.1 Result of Experiment 1**

Empty Crucible=**333.20g**

Start weight = **343.20g**

End weight = 333.87-333.20 (crucible) = **0.67 g**

Mass of residue=  $0.67/10 \times 100=6.7\%$  **w/w**

Percentage reduction in mass=  $(100-3.3) = 93.3\%$

#### **6.3.7.2 Result of Experiment 2**

Empty Crucible=**333.20g**

Start weight = **343.20**

End weight = 333.70-333.20 (crucible) = **0.5g**

Mass of residue=  $0.5/10 \times 100=5\%$  **w/w**

Percentage reduction in mass=  $(100-5) = 95.0\%$

### 6.3.7.3 Result of Experiment 3

Empty Crucible=**333.20g**

Start weight = **343.20**

End weight = 333.80-333.20 (crucible) = **0.6g**

Mass of residue=  $0.6/10 \times 100=6\%$  w/w

Percentage reduction in mass=  $(100-6) = 94.0\%$

*Table 6.10: Mass change of each napkin/paper waste sample in response to microwave pyrolysis treatment*

Experiment	1	2	3
Start mass (g)	10.00g	10.00g	10.00g
End mass (g)	0.67	0.5	0.6
Total loss (g)	9.33	9.50	9.40

Table 6.10 shows the start and final mass of the napkin/paper waste. The samples were not pre-dried. 10g mass were used for the experiment and a mean reduction of 94.1% was observed, with a standard deviation of 1%.

## 6.4 Chapter Summary

In this chapter the results of the three different categories of waste sent out to external laboratory Knight Energy Limited for analysis are discussed. Results of the sample moisture measurements are presented. Results from the energy dispersive X-ray (EDX) measurement were explained in detailed based on the different category of the waste. Three repetition of results of the pyrolysis/gasification experiments presented and discussed. Chapter Seven will explain about the conclusion and future work.

## CONCLUSIONS AND FUTURE WORK

### 7 : Conclusion

A 2.45GHz microwave plasma gasification system, operating at 1kW with argon as the plasma gas, has been used to produce syngas from waste samples from a city centre, fast food restaurant. The syngas could potentially be used as a source of energy for heating or electricity. The focus of the work has been to investigate the potential of this approach for dealing with waste from city centre restaurants using a small on-site system. This thesis explains the problems that currently arise due to the amount of food waste being sent to landfill. Tests have shown that the amount of landfill waste would be reduced by approximately 94% if this method were used, which addresses the aim of this work. Three different waste categories were investigated: mixed food, napkin/paper and fries/chips. The 10g samples were not dried prior to testing, as this was considered to be unrealistic in the real world.

The design of the microwave plasma cavity was performed using the simulation software, COMSOL. The cavity consists of a tapered waveguide section that is shorted at one end. When power is applied to the open end, a stationary wave occurs at the tapered position that produces a large electric field. This, in addition to a tapered gas nozzle placed inside the cavity, enhances the field enough to produce a self-striking plasma when argon is applied to the nozzle. The best argon flow rate was found to be 1.5 litres/minute. Nitrogen was used to keep the plasma cavity clear of smoke, vapours and other hot gas. The best nitrogen flow rates were found to be

around 2 litres/minute, although 5 litres/minute was used to dilute the exhaust gases prior to analysis. The nitrogen was applied through a connection in the waveguide flange, next to the microwave window, and flowed through the plasma cavity. They exited through the same aperture as the plasma jet and entered the gasifier. The combination of the argon and nitrogen purged the gasifier of oxygen. The pressure in the gasifier was held at 200mbar, and the tuning system tracking the minimum reflected power for efficiency.

The microwave generated plasma interacts with the samples to create syngas. Syngas production was recorded using a Quintox gas analyser that measured CO, CO<sub>2</sub> and O<sub>2</sub>. The data was captured every 10s during testing using a PC running a custom-built LabVIEW program. This program was also used to set the microwave output power and record the reflected power and temperatures using National Instruments cDAQ modules with analogue to digital converters. The CO and H<sub>2</sub> in syngas could be used as a fuel to offset the cost of running the plasma.

The ashes produced by the tests were investigated using SEM/EDX analysis. The appearance of carbon in the ash and in the elemental weight percentages suggests that the system can be improved further.

## 7.1 Future Work

The box reactor system can only deal with small samples (10-30g). Further development would be required to produce a system that could manage the amounts generated by a busy restaurant, with a larger scale reactor required.

Modifications would also be required to allow continuous feeding of waste into the reactor. Another problem that needs to be addressed for long term use is the build-up of dirt and condensation on the quartz window. The window is used to prevent gases and smoke from reaching the isolator and magnetron. Even with the nitrogen flowing, condensation can occur after the test is complete if the nitrogen is turned off while the gasifier is still warm. Condensation on the window interferes with microwave transmission and this will make the plasma difficult to strike. Dirt on the window can cause the window to get hot and this can lead to a failure of the window.

The tuning required to match the impedance seen by the magnetron to the impedance presented by the plasma cavity is currently performed manually. This impedance is a function of the length of the plasma, which in turn depends on the microwave power and the plasma gas flow rate. Automated tuners are available to perform this task and these would ultimately be required in a commercial microwave gasifier system. Reducing the reflected power would improve efficiencies, but the problem with automatic tuning is that it would also respond to an instability, and this could result in damage to the system components such as the microwave window. Software would need to be written that identifies instability problems and overrides the tuning if required. Further research to monitor the link between reflected power and instabilities would be necessary.

Based on the EDX results of the ash, it has potential use in building materials such as cement/concrete, ceramics and glass/glass-ceramics [90, 91].

Other materials such as clinical and hazardous waste could be investigated using this system.

## 8 : References

1. Lipinski, B., et al., *Reducing food loss and waste*. World Resources Institute Working Paper, June, 2013.
2. Hollins, O., *Overview of waste in the UK Hospitality and Food Service Sector*, in *An Overview of Waste in the UK Hospitality and Food Service Sector*. 2013, WRAP Banbury.
3. Association, S.R., *Too good to waste: Restaurant food waste survey report*. Sustainable Restaurant Association, UK, 2010.
4. Melikoglu, M., C. Lin, and C. Webb, *Analysing global food waste problem: pinpointing the facts and estimating the energy content*. Open Engineering, 2013. **3**(2).
5. Griffiths, P. and K. Lewis. *Development of a Standardised Methodology for Resource Flow Analysis and its Application to Sub-National Regions*. in *Paper delivered at the Clean Air Congress, London*. 2004.
6. Eggleston, S., et al., *Intergovernmental Panel on Climate Change*. IPCC Guidelines for National Greenhouse Gas Inventories, 2006.
7. Burnley, S., *The impact of the European landfill directive on waste management in the United Kingdom*. Resources, Conservation and Recycling, 2001. **32**(3-4): p. 349-358.
8. Gendebien, A., et al., *Landfill gas from environment to energy*. 1992, Commission of the European Communities.
9. Melikoglu, M., C.S.K. Lin, and C. Webb, *Analysing global food waste problem: pinpointing the facts and estimating the energy content*. Central European Journal of Engineering, 2013. **3**(2): p. 157-164.
10. Lupa, C.J., et al., *Gas evolution and syngas heating value from advanced thermal treatment of waste using microwave-induced plasma*. Renewable energy, 2013. **50**: p. 1065-1072.
11. Kathirvale, S., et al., *Energy potential from municipal solid waste in Malaysia*. Renewable energy, 2004. **29**(4): p. 559-567.
12. Ahmed, I. and A. Gupta, *Syngas yield during pyrolysis and steam gasification of paper*. Applied energy, 2009. **86**(9): p. 1813-1821.
13. Caton, P., et al., *Energy recovery from waste food by combustion or gasification with the potential for regenerative dehydration: A case study*. Energy Conversion and Management, 2010. **51**(6): p. 1157-1169.
14. Chu, S. and A. Majumdar, *Opportunities and challenges for a sustainable energy future*. nature, 2012. **488**(7411): p. 294.
15. Ngô, C. and J. Natowitz, *Our energy future: resources, alternatives and the environment*. 2016: John Wiley & Sons.

16. Johari, A., et al., *Economic and environmental benefits of landfill gas from municipal solid waste in Malaysia*. Renewable and Sustainable Energy Reviews, 2012. **16**(5): p. 2907-2912.
17. Lin, C.S.K., et al., *Food waste as a valuable resource for the production of chemicals, materials and fuels. Current situation and global perspective*. Energy & Environmental Science, 2013. **6**(2): p. 426-464.
18. Haug, R.T., *The practical handbook of compost engineering*. 1993: CRC Press.
19. Stuart, T., *Waste: uncovering the global food scandal*. 2009: WW Norton & Company.
20. Banks, C.J., et al., *Anaerobic digestion of source-segregated domestic food waste: performance assessment by mass and energy balance*. Bioresource technology, 2011. **102**(2): p. 612-620.
21. Bridgwater, A.V., *Renewable fuels and chemicals by thermal processing of biomass*. Chemical Engineering Journal, 2003. **91**(2-3): p. 87-102.
22. Kessel, D.G., *Global warming—facts, assessment, countermeasures*. Journal of Petroleum Science and Engineering, 2000. **26**(1): p. 157-168.
23. Demirbas, A., *Combustion characteristics of different biomass fuels*. Progress in energy and combustion science, 2004. **30**(2): p. 219-230.
24. Nordell, B., *Global warming is large-scale thermal energy storage*, in *Thermal Energy Storage for Sustainable Energy Consumption*. 2007, Springer. p. 75-86.
25. Schwartz, S.E., *Does fossil fuel combustion lead to global warming?* Energy, 1993. **18**(12): p. 1229-1248.
26. Boehman, A.L. and O.L. Corre, *Combustion of Syngas in Internal Combustion Engines*. Combustion Science and Technology, 2008. **180**(6): p. 1193-1206.
27. Wallace, H., M.A. Pollack, and A.R. Young, *Policy-making in the European Union*. 2015: Oxford University Press, USA.
28. Tonglet, M., P.S. Phillips, and A.D. Read, *Using the Theory of Planned Behaviour to investigate the determinants of recycling behaviour: a case study from Brixworth, UK*. Resources, conservation and recycling, 2004. **41**(3): p. 191-214.
29. Williams, P.T., *Waste treatment and disposal*. 2013: John Wiley & Sons.
30. Karousakis, K. and E. Birol, *Investigating household preferences for kerbside recycling services in London: A choice experiment approach*. Journal of Environmental Management, 2008. **88**(4): p. 1099-1108.
31. Price, J.L., *The landfill directive and the challenge ahead: demands and pressures on the UK householder*. Resources, Conservation and recycling, 2001. **32**(3): p. 333-348.
32. Marasini, R., et al., *An investigation into the logistics and management of uncontaminated soil exchange in the Southern region of the UK*. 2012.
33. Nayono, S.E., *Anaerobic digestion of organic solid waste for energy production*. Vol. 46. 2010: KIT scientific Publishing.

34. Santoianni, D.A., et al. *Power from Animal Waste—Economic, Technical, and Regulatory Landscape in the United States*. in *Journal of Electric Utilities Environmental Conference*. 2008.
35. McKendry, P., *Energy production from biomass (part 3): gasification technologies*. *Bioresource technology*, 2002. **83**(1): p. 55-63.
36. Foley, G. and G. Barnard, *Biomass gasification in developing countries- Technical Report*. International Institute for Environment and Development, Earthscan, UK, 1983.
37. Basu, P., *Biomass gasification and pyrolysis: practical design and theory*. 2010: Academic press.
38. Protocol, K., *United Nations framework convention on climate change*. Kyoto Protocol, Kyoto, 1997. **19**.
39. Grubb, M., C. Vrolijk, and D. Brack, *The Kyoto Protocol. A guide and assessment*. 1999.
40. Bridgwater, A.V., *Renewable fuels and chemicals by thermal processing of biomass*. *Chemical Engineering Journal*, 2003. **91**(2): p. 87-102.
41. Fabry, F., et al., *Waste gasification by thermal plasma: a review*. *Waste and Biomass Valorization*, 2013. **4**(3): p. 421-439.
42. Ciferno, J.P. and J.J. Marano, *Benchmarking biomass gasification technologies for fuels, chemicals and hydrogen production*. US Department of Energy. National Energy Technology Laboratory, 2002.
43. Belgiorno, V., et al., *Energy from gasification of solid wastes*. *Waste management*, 2003. **23**(1): p. 1-15.
44. Overend, R.P., *Energy From Biomass*. *Renewable Energy Sources Charged With Energy from the Sun and Originated from Earth-Moon Interactions- Volume I*, 2009. **8**: p. 47.
45. Demirbas, A., *Current technologies for the thermo-conversion of biomass into fuels and chemicals*. *Energy Sources*, 2004. **26**(8): p. 715-730.
46. Maschio, G., C. Koufopoulos, and A. Lucchesi, *Pyrolysis, a promising route for biomass utilization*. *Bioresource technology*, 1992. **42**(3): p. 219-231.
47. Kabalan, B., et al. *Real-time Optimisation of a Microwave Plasma Gasification System*. in *Journal of Physics: Conference Series*. 2011. IOP Publishing.
48. Shafizadeh, F., *Basic principles of direct combustion*, in *Biomass conversion processes for energy and fuels*. 1981, Springer. p. 103-124.
49. Igoni, A.H., et al., *Designs of anaerobic digesters for producing biogas from municipal solid-waste*. *Applied energy*, 2008. **85**(6): p. 430-438.
50. Williams, A., M. Pourkashanian, and J. Jones, *Combustion of pulverised coal and biomass*. *Progress in Energy and Combustion Science*, 2001. **27**(6): p. 587-610.
51. Allen, B., et al., *Ultra wideband antennas and propagation for communications, radar and imaging*. 2006: John Wiley & Sons.

52. Chang, K., *RF and microwave wireless systems*. Vol. 161. 2004: John Wiley & Sons.
53. White, J.F., *High frequency techniques: an introduction to RF and microwave engineering*. 2004: John Wiley & Sons.
54. Cheng, P.-K., *NeXtRAD antenna design: X-Band dual polarised conical horn antenna*. 2016, University of Cape Town.
55. Weiland, T., *Time domain electromagnetic field computation with finite difference methods*. International Journal of Numerical Modelling: Electronic Networks, Devices and Fields, 1996. **9**(4): p. 295-319.
56. Martín, R.G., *Electromagnetic field theory for physicists and engineers: Fundamentals and Applications*. Grupo de Electromagnetismo de Granada, 2006.
57. Shevgaonkar, R., *Electromagnetic waves*. 2005: Tata McGraw-Hill Education.
58. Graham, B., *Technological plasmas*. Physics World, 2001. **14**(3): p. 31.
59. Boulos, M.I., P. Fauchais, and E. Pfender, *Thermal plasmas: fundamentals and applications*. 2013: Springer Science & Business Media.
60. Al-Shamma'a, A., et al., *Design and construction of a 2.45 GHz waveguide-based microwave plasma jet at atmospheric pressure for material processing*. Journal of Physics D: Applied Physics, 2001. **34**(18): p. 2734.
61. Fridman, A. and L.A. Kennedy, *Plasma physics and engineering*. 2004: CRC press.
62. Grill, A., *Cold plasma in materials fabrication*. Vol. 151. 1994: IEEE Press, New York.
63. Howard, J., *Introduction to plasma physics*. Plasma Research Laboratory, Research School of Physical Sciences and Engineering, Australian National University, 2002.
64. Benford, J., J.A. Swegle, and E. Schamiloglu, *High power microwaves*. 2015: CRC Press.
65. Schutze, A., et al., *The atmospheric-pressure plasma jet: a review and comparison to other plasma sources*. IEEE transactions on plasma science, 1998. **26**(6): p. 1685-1694.
66. Conrads, H. and M. Schmidt, *Plasma generation and plasma sources*. Plasma Sources Science and Technology, 2000. **9**(4): p. 441.
67. Hughes, A. and J. McMillen, *Inelastic and elastic electron scattering in argon*. Physical Review, 1932. **39**(4): p. 585.
68. Jonkers, J., et al., *On the differences between ionizing helium and argon plasmas at atmospheric pressure*. Plasma Sources Science and Technology, 2002. **12**(1): p. 30.
69. Sheppard, B.S., et al., *Helium-argon inductively coupled plasma for plasma source mass spectrometry*. Journal of Analytical Atomic Spectrometry, 1990. **5**(8): p. 697-700.

70. Jankowski, K. and A. Jackowska, *Spectroscopic diagnostics for evaluation of the analytical potential of argon+ helium microwave-induced plasma with solution nebulization*. Journal of Analytical Atomic Spectrometry, 2007. **22**(9): p. 1076-1082.
71. Uchida, H., *Effects of Central Argon Flow Rate on Characteristics of Inductively Coupled Plasma*. Spectroscopy Letters, 1981. **14**(10): p. 665-674.
72. Djebabra, D., O. Dessaux, and P. Goudmand, *Coal gasification by microwave plasma in water vapour*. Fuel, 1991. **70**(12): p. 1473-1475.
73. Kanilo, P., et al., *Microwave plasma combustion of coal*. Fuel, 2003. **82**(2): p. 187-193.
74. Tang, L. and H. Huang, *Plasma pyrolysis of biomass for production of syngas and carbon adsorbent*. Energy & Fuels, 2005. **19**(3): p. 1174-1178.
75. Kamei, O., et al., *Brown coal conversion by microwave plasma reactions under successive supply of methane*. Fuel, 1998. **77**(13): p. 1503-1506.
76. Scott, R.M., *Chemical hazards in the workplace*. 1989: CRC Press.
77. Williams, C., *Introduction to sensors*. J. Res. Natl. Inst. Stand. Technol, 1998. **103**: p. 163.
78. National Instruments. *NI 9401 Specifications*. 2017 [cited 2017; Available from: <http://www.ni.com/documentation/en/c-series-digital-module/latest/9401/specs/>].
79. National Instruments. *NI 9211 Datasheet*. [cited 2017; Available from: [www.ni.com/nisearch/app/main/p/ap/tech/lang/en/pg/1/sn/ssnav:spc/aq/pmdmid:122163/](http://www.ni.com/nisearch/app/main/p/ap/tech/lang/en/pg/1/sn/ssnav:spc/aq/pmdmid:122163/)].
80. National Instruments. *NI 9263 Specifications*. [cited 2017; Available from: <http://www.ni.com/documentation/en/c-series-voltage-output-module/latest/9263/specs/>].
81. National Instruments. *NI 9205 Specifications*. [cited 2017; Available from: <http://www.ni.com/documentation/en/c-series-voltage-input-module/latest/9205/specs/>].
82. Kane Keison. *Kane-9106 Quintox Upgradeable Combustion Analyser*. [cited 2017; Available from: [http://www.keison.co.uk/kane\\_9106.shtml](http://www.keison.co.uk/kane_9106.shtml)].
83. Tikuisis, P., et al., *Rate of formation of carboxyhemoglobin in exercising humans exposed to carbon monoxide*. Journal of Applied Physiology, 1992. **72**(4): p. 1311-1319.
84. Safety, O. and H. Administration, *Occupational safety and health guideline for carbon monoxide*. 2003.
85. Moore, J., *Wood properties and uses of Sitka spruce in Britain*. 2011: Forestry Commission.
86. Ciolkosz, D., B. Miller, and R. Wallace, *Characteristics of biomass as a heating fuel*. Renewable and Alternative Energy Fact Sheet, 2010: p. 1-2.
87. Lindeburg, M.R., *Civil engineering reference manual for the PE exam*. 2012: [www.ppi2pass.com](http://www.ppi2pass.com).

88. Sairem. *GMP 60K SM 56T400 FST 3 IR*. [cited 2017; Available from: <https://www.sairem.com/products/generators-standard-components-measurement/the-generators/>].
89. Nzihou, J.F., et al., *Using Dulong and Vandralk Formulas to Estimate the Calorific Heating Value of a Household Waste Model*. *Int. J. Sci. Eng. Res*, 2014. **5**(1): p. 1878-1883.
90. Ferreira, C., A. Ribeiro, and L. Ottosen, *Possible applications for municipal solid waste fly ash*. *Journal of hazardous materials*, 2003. **96**(2-3): p. 201-216.
91. Smol, M., et al., *The possible use of sewage sludge ash (SSA) in the construction industry as a way towards a circular economy*. *Journal of Cleaner Production*, 2015. **95**: p. 45-54.